ISOLATION OF LEUKEMIC STEM CELLS BY USING A LENTIVIRAL REPORTER SYSTEM

MASTER'S THESIS

in

Medicine with Industrial Specialization
Biomedicine

Title:	Isolation of Leukemic Stem Cells by using a Lentiviral Reporter System
Project period:	02/09-2019 - 05/08-2020
Semesters and group:	9th and 10th semester Medicine with Industrial Specialization, group 9044
Intern supervisor:	Cristian Pablo Alejandro Pennisi
Faculty:	University of Aalborg Department of Health Science and Technology Fredrik Bajers Vej 7 D2, 9220 Aalborg East, Denmark
Extern supervisor:	Krister Wennerberg
Company:	Biotech Research and Innovation Centre, BRIC Ole Maaløes Vej 5, 2200 Copenhagen N, Denmark University of Copenhagen Faculty of Health and Medical Sciences
Number of pages:	55
Characters with spaces:	88,733
Author:	

Maja Balling Zacher Sørensen - 20154184

Preface

The present master's thesis was carried out in collaboration with Professor Krister Wennerberg at Biotech Research and Innovation Centre, BRIC, University of Copenhagen, from early September 2019 till end of February 2020 and again from end May till early August 2020. I would like to express my gratitude to Professor Krister Wennerberg for welcoming me in his laboratory. Additionally, a great thank to all the people in Wennerberg group, especially Ph.D. student Josephine Amalie Meilstrup for advice and guidance throughout the project. I would also like to thank my internal supervisor at Aalborg University, Associate Professor Pablo Pennisi, who also has been giving excellent advice and guidance throughout this project.

Abstract

Leukemic stem cells (LSCs) are mutated hematopoietic stem or progenitor cells that can initiate acute myeloid leukemia (AML). LSCs are a source of relapse, as they are often more resistant to conventional chemotherapies and therefore, the identification of drugs that effectively target LSCs is of great importance for establishing more effective treatments towards AML. However, there is no simple way to identify the LSCs since the immunophenotype varies from case to case. The ERG+85 enhancer promoter relates to the endogenous ERG expression which correlates to stemness state. A reporter system based on this has recently been shown potential for the identification of cellular stemness. The overall objective in the present thesis was to implement a novel method for identifying LSCs using a lentiviral stemness reporter system, which could allow exploring compounds that target LSCs in AML. In order to achieve this, a lentivirus was produced containing the vector pMIN-ERG+85. The vector contains a constitutive green fluorescent protein (GFP) reporter and a blue fluorescent protein (BFP) gene under the ERG+85 enhancer promoter. Plasmids for lentiviral production was transformed into competent *Escherichia coli* XL1-blue cells with either pMIN-ERG+85 or the control vector pMIN. HEK 293T cells were then transfected with the plasmids to produce lentivirus, either containing pMIN-ERG+85 or pMIN. The AML cell lines Kasumi-1, KG-1, and MOLM-13 were transduced with the lentiviral vectors. Infected cells were sorted by FACS and long term cultured, in order to expand the number of cells for drug screenings. Infected cells were repeatedly assessed by flow cytometry. Results showed that transduction was enhanced by the use of polybrene transduction reagent, that lentiviral vectors were able to infect Kasumi-1 and MOLM-13 but not KG-1, and that transduction were more efficient with pMIN than pMIN-ERG+85. Moreover, showed infected cells a higher BFP signal in the control vector, pMIN, compared to pMIN-ERG+85 vector suggesting leaky promoter activity of the mCMV promoter. The drug screen assessments could not be implemented due to time restrictions, and it can be concluded that further investigations are needed regarding the higher BFP signal in the control vector.

Table of Contents

Abbreviations

AML	Acute myeloid leukemia
BFP	Blue fluorescent protein
bp	Base pair
BM	Bone marrow
C/EBP	CCAAT/enhancer-binding protein
CLP	Common lymphoid progenitor
CMP	Common myeloid progenitor
CR	Complete remission
CXCL12	C-X-C Motif Chemokine Ligand 12
DMEM	Dulbecco's Modified Eagle Medium
EC	Endothelial cell
ERG	E-twenty-six (ETS)-related gene
FAB	French-American-British
FACS	Fluorescence activated cell sorting
FBS	Fetal bovine serum
FLT3	FMS-like tyrosine kinase 3
FSC	Forward scatter
GFP	Green fluorescent protein
GMP	Granulocyte-monocyte progenitor
GO	Gemtuzumab ozogamicin
HEK	Human embryonic kidney
HSC	Hematopoietic stem cell
LB	Lysogeny broth
LMPP	Lymphoid-primed multipotent progenitor
LSC	Leukemic stem cell
mCMV	Minimal cytomegalovirus
MEP	Megakaryocyte-erythrocyte progenitor
MHC	Major histocompatibility complex
MOI	Multiplicity of infection
MPP	Multipotent progenitor

MSC	Mesenchymal stem cell
NK	Natural killer
NPM1	Nucleophosmin 1
PBS	Phosphate buffered saline
Pen-strep	Penicillin/streptomycin
RUNX1	Runt-related transcription factor 1
rpm	Round per minute
RPMI	Roswell Park Memorial Institute
SSC	Side scatter
TU	Transducing unit
VSV-G	Vesicular stomatitis virus glycoprotein
WHO	World Health Organization

1. Introduction

According to the American Cancer Society, the incidence of leukemia in 2020 is expected to reach approximately 60,000 in the US (1). Acute myeloid leukemia (AML) is one of the most common forms of leukemia, with an estimate of 21,000 new cases per year in the US. Of all subtypes of leukemia, including acute lymphocytic leukemia, chronic myeloid leukemia, and chronic lymphocytic leukemia, AML accounts for the highest percentage of leukemia related deaths with 62%. This type of malignancy can affect all age groups, however it primarily affects the elderly population which is evident by the increase in incidens with age, and the average age at diagnosis being 68 years (2). AML is a highly aggressive blood malignancy characterized by abnormal growth caused by acquired genetic alterations in the hematopoietic stem cells (HSCs), leading to accumulation of immature myeloid progenitor cells in the bone marrow (BM), peripheral blood, and other tissues (3). The expansion of immature cells from the myeloid lineage occurs at the expense of normal hematopoiesis, in which an array of clinical manifestations will arise including fatigue and shortness of breath, recurrent infections, and an increased bleeding tendency due to anemia, neutropenia, and thrombocytopenia, respectively (4). Without treatment, the patient will usually die within a few months of diagnosis. Even after obtaining complete remission (CR) after treatment with aggressive multiagent chemotherapy and allogeneic stem cell transplantation, relapses are frequent, and only 24% is alive after five years (2).

1.1 Adult hematopoiesis and stem cell niches

Hematopoiesis is the process of which all mature, circulating blood cells are formed and happens within the BM. The hematopoiesis is a hierarchal system with the HSCs at the apex. Two fundamental characteristics define the HSC: the feature to undergo self-renewal, and the ability to differentiate into specialized blood cells, an ability known as multipotency (5). Most HSCs are dormant, being in the G0 phase of the cell cycle. When an HSC enters the cell cycle, they either undergo symmetric division where two HSCs are formed or an asymmetric division where one HSC and one progenitor cell are formed (6). To give rise to circulating, mature blood cells, the HSCs must first differentiate into multipotent progenitor (MPP) cells followed by differentiating into either a common myeloid progenitor (CMP) cell or a lymphoid-primed multipotent progenitor (LMPP) cell. The CMP cell can further give rise to either a

megakaryocyte-erythrocyte progenitor (MEP) cell or a granulocyte-monocyte progenitor (GMP) cells. The LMPP cell, on the other hand, can give rise to a GMP cell or a common lymphoid progenitor (CLP) cell (5). A schematic overview of normal adult hematopoiesis is shown in Figure 1.

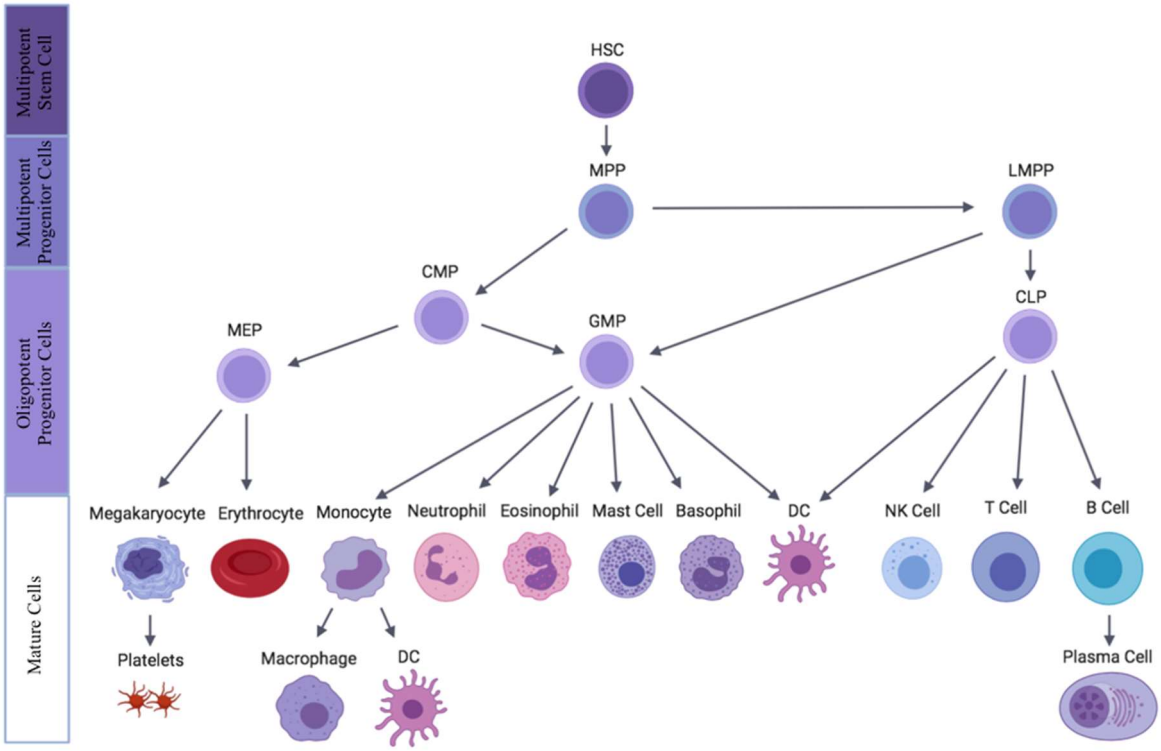

Figure 1. Illustration of normal adult hematopoiesis. Multipotent progenitor cell (MPP). Lymphoid-primed multipotent progenitor (LMPP). Common myeloid progenitor (CMP). Megakaryocyte-erythrocyte progenitor (MEP). Granulocyte-monocyte progenitor (GMP). Common lymphoid progenitor (CLP). Dendritic cell (DC) and natural killer (NK) cell. Inspired from (7).

The regulation of hematopoiesis is a highly interconnected regulatory network located in the specialized microenvironment in the BM, the stem cell niche. The niche is responsible for promoting the maintenance of HSCs, including quiescence, proliferation, differentiation, and migration. Within the stem cell niche different types of cells, such as bone cells (osteoblasts and osteoclasts), and mesenchymal stem cells (MSCs), directly or indirectly interact with HSCs, by exchanging molecular signals and secreting growth factors and chemokines.

Histologically, two distinct niches within the BM are postulated, the osteoblastic (endosteal) and the vascular niche, which cooperate in order to maintain hematopoiesis (8). Most HSCs reside in endosteal niche, closely to the sinusoidal area (9). The endosteal niche is located at

the inner surface of the bone cavity, containing different cells types, i.e. abundant bone-forming osteoblasts, and bone degrading osteoclasts, which modulate specialized features. For instance, when an HSC binds via its receptor, Tie-2, to Ang-1 on osteoblasts, an enhanced adhesion contributes to the maintenance of HSC quiescence. Interaction between Jag-1 on osteoblasts and its associated receptor NOCTH placed on HSCs, on the other hand, can provide expansion of HSCs (8). However, osteoblasts can also regulate the HSC pool size by expressing osteopontin leading to inhibition of HSC proliferation and promote apoptosis. The C-X-C Motif Chemokine Ligand 12 (CXCL12) produced by osteoblasts, among other stromal cells, is one of the most important chemoattractants for HSCs. Mice lacking in CXCL12 or its receptor CXC4 show aberrant BM engraftment by HSCs suggesting that CXCL12-CXCR4 chemokine signaling is playing an essential role in HSC maintenance (10). Besides osteoblasts, osteoclasts are also found in the endosteal niche as they form the cavities that organize the endosteal niche (8). The vascular niche is localized closely to the osteoblastic niche. The niche contains different types of cells, i.e. CXCL12-abundant reticular cells, MSCs and endothelial cells (ECs). Interactions between HSCs and ECs, further induce the HSCs functions of self-renewal and differentiation (8). From being in a dormant state in the endosteal niche, the hematopoietic progenitor cells penetrate the ECs entering the vascular niche, which allows further differentiation. Eventually the progenitors leave the BM and join the circulation system to become mature blood cells to perform their primary function (9).

1.2 Pathology of AML

Myeloid differentiation block is a hallmark of AML. This is linked to genomic mutations or translocations in genes affecting normal hematopoiesis. Mutations that disturb transcriptional activity of essential differentiations-inducing transcription factors are believed to be one of the reasons for development of AML (11,12). Even though the number of alterations in AML compared to many solid tumors is lesser, it still accounts for a genetically heterogeneous malignancy with a complex pathophysiology (13). Current advances in molecular genetics have led to a greatly improved understanding of the underlying mechanisms in regard to AML, however, some parts of the disease pathology remain unclear. A schematic overview of the transition from HSCs and progenitor cells into leukemic stem cells (LSCs) is shown in Figure 2.

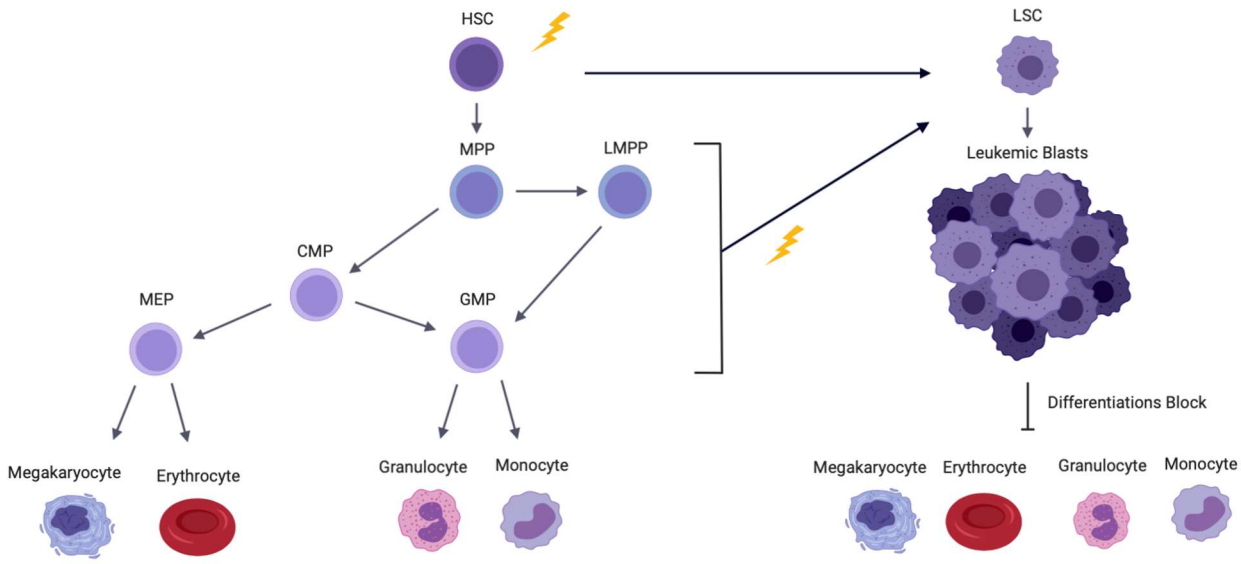

Figure 2. Overview of cell of origin and its transition into LSC. Inspired from (14).

Genetic mutations involved in leukemogenesis are linked to several cellular features including ligand-receptor interaction, signal transduction, cell cycle and apoptosis. Underlying oncogenic events leading to AML are often divided into two classes of mutations. Class I mutations contribute to proliferative and survival signals in advantage to blast cells, characteristically as a result of abnormal activation of signal pathways. On the other hand, class II mutations have an impact on differentiation as these mutations interfere with transcription factors. The interplay among these classes of mutations can lead to development of LSCs (15).

1.2.1 Common genetic mutations in AML

One of the most common mutations in AML occurs in the gene encoding for Nucleophosmin 1 (*NPM1*). Approximately 35% of all AML cases carries a mutation in the *NPM1* gene, for patients with normal karyotype it is up to 60%. NPM1 is a nucleolar shuttling phosphoprotein regulating multiple cellular events, such as DNA repair, apoptosis and genome stability (13). NPM1 constantly shuttles between the nucleus and cytoplasm in order to preserve cellular homeostasis. NPM1 is important in regulating the cell cycle. For instance, once a cell is exposed to stress, the level of NPM1 increases, leading to upregulated transcriptional activity of p53 and MDM2 proteins. NPM1 binds MDM2 and thereby acting as a negative regulator on p53-MDM2 interaction. The mutations and translocations in the *NPM1* gene found in AML cause

cytoplasmatic dislocation of the NPM1 protein, and it thereby loses its ability to perform its function (13). The dislocation of NPM1 also leads to an aberrant interaction with the myeloid transcription factor PU.1, which is a key transcription factor of the myeloid linage. When mutated cytoplasmic NPM1 interacts with this transcription factor it sequesters PU.1 in the cytoplasm, thereby blocking myeloid differentiation (13,16).

Another common mutation that occurs in AML is within the FMS-like tyrosine kinase 3 (*FLT3*). The *FLT3* gene encodes a tyrosine kinase receptor, present on HSCs and myeloid progenitors (15). When FLT3 binds to its extracellular ligand (FLT3 ligand) a homodimerization of the receptor occurs allowing for conformational change resulting in phosphorylation and activation of the cytoplasmic tyrosine kinase domain. When the receptor becomes active a downstream cascade of signal pathways are initiated, such as RAS and PI3K pathways, eventually leading to survival, proliferation, differentiation (17). The most common mutations in *FLT3* found in AML are either an internal tandem duplication (FLT3-ITD) or a point mutation in the kinase domain. These mutations cause constitutive activation of the FLT3 kinase and hyperactivation of the downstream intracellular signaling networks (15). Moreover, *FLT3* mutations can provide repression of CCAAT/enhancer-binding protein (C/EBP) and PU.1 expression, indicating that they also supply a differentiation block of the myeloid linage (18). Patients with a *FLT3* mutation have a worse prognosis compared to patients without this mutation (15).

Besides gene mutations, genetic translocation can contribute to leukemogenesis, as oncogenic fusion products can cause aberrant transcriptional activity (11) and there are more than 700 known translocations so far in AML (19). One of the most frequent translocations found in AML is between chromosome 8 and 21, t(8;21). The translocation leads to a fusion gene consisting of the runt-related transcription factor 1 (RUNX1) gene on chromosome 21 and the ETO gene located on chromosome 8, resulting in the oncogenic fusion protein RUNX1/ETO (20). The RUNX1/ETO fusion protein can interrupt transcriptional activity of essential myeloid transcription factors such as PU.1 and GATA1 by downregulating their gene expression, leading to differentiation arrest (21). Patients diagnosed with this translocation are associated with a favorable outcome. Overall, the constellation of alterations in AML has a great responsibility in the disease prognosis due to the impact on treatment responsiveness (22).

1.2.2 Classification and diagnosis of AML

There are two primary systems used to diagnostically classify AML, dividing the disease into different subtypes. The French-American-British (FAB) classification developed in the 1970s divides AMLs into subtypes (M0-M7) based on a morphologic assessment involving the type of cell in which the leukemia arises from and the maturity of the cells (23). A newer classification system is compiled by the World Health Organization (WHO) by means of new insights of the genomic landscape of AML (24). Both classification systems are shown in Table 1.

Table 1. Overview of the two different classification systems of AML. Left table: The French-American-British (FAB) classification system is presented (23)*. Right table: A simplified version of WHO classifications are presented* (24)*.*

FAB Classification	
M0	Undifferentiated acute myeloblastic leukemia
M1	Acute myeloblastic leukemia with minimal maturation
M2	Acute myeloblastic leukemia with maturation
M3	Acute promyelocytic leukemia (APL)
M4	Acute myelomonocytic leukemia
M4 Eos	Acute myelomonocytic leukemia with eosinophilia
M5	Acute monocytic leukemia
M6	Acute erythroid leukemia
M7	Acute megakaryoblastic leukemia

WHO Classification
AML with recurrent genetic abnormalities
AML with myelodysplasia related changes
Therapy-related myeloid neoplasms
AML, not otherwise specified
Myeloid sarcoma
Myeloid proliferations associated with Down syndrome
Myeloid neoplasms with germline predisposition
Acute leukemias of ambiguous lineage

In order to classify and diagnose AML, morphological, immunophenotypic, cytogenic and molecular genetic examination are necessitated. The diagnosis of AML can be confirmed when the blood or BM contains at least 20% blasts, with the exception of for AML with t(8;21), t(15;17), t(16;16) or inv(16). To confirm whether the blasts are of the myeloid lineage, an immunophenotypic investigation is performed to determine surface markers, such as CD33, CD34 and CD117. The cytogenetic analysis is performed to investigate genetic abnormalities, such as chromosomal rearrangements. Moreover, molecular genetic testing can give an indication of any genetic mutations involved in the disease (25).

Besides diagnostics, AML have been classified according to risk stratification for a standardized prognostic purpose (25). As seen in Table 2, AML can be distinguished into three

categories based on genetic abnormalities. The table provides a rough overview of genetic risk stratification and can be a helpful regarding choice of treatment (26).

Table 2. 2017 European LeukemiaNet risk stratification by genetics (25).

Risk category	Genetic abnormalities
Favorable	t(8;21)(q22;q22.1)/*RUNX1-RUNX1T1* inv(16)(p13.1q22) or t(16;16)(p13.1;q22)/CBFB-MYH11 Mutated *NPM1* without FLT3-ITD/FLT3-ITD^{low} Biallelic mutated *CEBPA*
Intermediate	Mutated *NPM1* and FLT3-ITD^{high} Wild-type *NPM1* without FLT3-ITD or with FLT3-ITD^{low} (without adverse risk genetic lesions) t(9;11)(p21.3;q23.3)/*MLLT3-KMT2A* Cytogenetic abnormalities not classified as favorable or adverse
Adverse	t(6;9)(p23;q34.1)/*DEK-NUP214* t(v;11q23.3)/*KMT2A* rearranged t(9;22)(q34.1;q11.2)/*BCR-ABL1* inv(3)(q21.3q26.2) or t(3;3)(q21.3;q26.2); *GATA2, MECOM*(EVI1) -5 or del(5q); -7;-17/abn(17p) Complex karyotype, monosomal karyotype Wild-type *NPM1* and FLT3-ITD^{high} Mutated *RUNX1* Mutated *ASXL1* Mutated *TP53*

1.3 Leukemic stem cells

LSC are mutated hematopoietic stem or progenitor cells being able to initiate leukemia (Figure 2). They harbor HSCs features, including self-renewal, quiescence and multipotency, and for a long time it was believed that LSCs shared the same phenotype as HSCs as being positive for CD34 and negative for CD38 surface markers. But studies in the more recent years have revealed that the LSCs are phenotypically diverse (27), and despite the majority of LSCs express $CD34^{+}/CD38^{-}$, it is nevertheless, observed that they can be found within all the CD34 and CD38 subpopulations. LSC have the ability to self-renew limitless and like HSCs, LSCs are mostly being dormant in the G0 phase of the cell cycle, which means that they are found to be resistant to traditional treatments (28). As HSCs and LSCs are sharing many of the same

features, it is challenging to eradicate the malignant cells without interrupt normal hematopoiesis and destroying HSCs (29).

1.3.1 ERG and ERG+85 function in HSCs and LSCs

Much research has been focusing on the transcriptional expression levels within AML, and it has been proven that the stem cell signature (stem-like program) also has an impact on clinical outcomes (30,31). The transcription factor ETS-related gene (ERG) is a member of both LSCs and HSCs signature and moreover, it is specifically associated with significantly worse outcome in AML (32). *ERG* is believed to be a powerful oncogene in hematological malignancies and even though *ERG* locus in some cases are rearranged, thus creating a fusion gene, high expression levels of ERG are most frequently seen in the absence of alterations related to its locus (33). In a study by Thoms et al. they discovered, that high ERG expression in T cell leukemia appears in the context of transcriptions factors including SCL, LMO2, LYL1, FLI1, ERG, and GATA3 binding to a specific enhancer within the *ERG* locus, namely the +85 kb downstream of the translation start site (34). Moreover, Diffner et al. showed that ERG expression in AML is related to activity of the same ERG promoter and +85 stem cell enhancer, and that it is regulated by a heptad of HSC transcription factors (33). Another research group that also investigated the ERG+85 enhancer identified it as a *"strong human HSCs-specific super enhancer"*. In that study, they wanted to utilize its activity to analyze the degree of stemness in HSCs and LSCs both *in vitro* and *in vivo*. They developed an experimental tool by integrating ERG+85 into a lentiviral reporter system that could be used as a marker for stemness when transducing both AML cell lines and patient-derived AML samples (35). This is the stemness reporter tool which will be investigated within this project.

1.3.2 Interplay between LSCs and the immune system

The first proof of the immune systems role in curing malignancies was reported back in 1950s by means of BM transplantation (36). Since then, much attention has gained within the immune system role to cancer and this has, among other things, led to HSC transplantation being a part of the standard treatment for AML patients. Moreover, it is now well described how the immune system is responding to cancer by the immune editing theory. The theory is built up upon three phases, where the first phase, elimination phase, describes the initial meeting between the innate and adaptive immune system and the malignant cells. The immune system can recognize

these cells at an early stage and eliminate them. If the malignant cells and the immune system, in the meantime, enters the next phase, equilibrium, the immune system try to prevent the malignant cells from expanding. Unfortunately, cancer cells can become unrecognizable for the immune system, and this will facilitate the cancer cells into the last phase, escape phase (19). The theory has been connected mostly to solid tumors, and a full understanding on the immune system's role in regard to AML somehow still remains questionable. The way the immune system recognizes the malignant cells is by means of neo-antigens present on the surface of malignant cells. Neo-antigens occur as a consequence of mutated genes. Antigen presenting cells can then take up the neo-antigen, followed by presenting it to naïve T cells in order to start an immune response. However, AML is known to have one of the lowest mutational burdens, with an average of 13 mutations per AML case, suggesting that LSCs are connected to low immunogenicity (19) as antigen presentation is limited. Besides loss of neoantigen expression, LSCs also harbor the ability to avoid immune response by creating a suppressive milieu. For instance, LSCs are found to express major histocompatibility complex (MHC) class I on their surface, and present neo-antigens to T cells but LSCs can prevent an immune response by expressing B7, CD80 and CD86. These molecules bind to cytotoxic T lymphocyte antigen 4 (CTLA-4) on T cells and thereby inhibit co-stimulatory signal (19).

Cytotoxic lymphocytes are also an important factor within the immune response; they express FasL on their surface and can induce apoptosis in Fas-carrying malignant cells. LSCs have a variable expression level of Fas on their surface, and interestingly, a study found, that FasL expression were higher in newly diagnosed AML patient samples compared to normal controls (37). This is another indication of escape from the immune system, as LSCs may kill cytotoxic lymphocytes. Moreover, NK cells are also an important factor within the immune system's interaction with malignant cells and it is well known that these cells can be activated when a down-regulation of MHC I occurs. LSCs are found to express MIC A, the ligand for NK cells receptor, NKG2D, however, in most cases, the expression is low (19), which can cause a low immune response from NK cells.

1.4 Treatment of AML

The purpose of treating AML patients is to achieve CR and thereby prolong overall survival. CR can be defined by the presence of ≤5% blasts is in the BM (25). The standard treatment of AML has not changed significantly within the last four decades (29), and induction therapy is

commonly referred to as "7+3" treatment, as it consists of three days with anthracycline and seven days with continuous cytarabine treatment. This therapy is usually offered to patients within intermediate and favorable prognosis groups, respectively (Table 2) and CR is achieved in approximated 60% of all cases. Once CR is achieved after induction therapy, post-remission therapy is initiated, aiming to eliminate residual LSCs, hence preventing relapses. Post-remission therapy also called consolidation therapy, consists of either intensive chemotherapy with cytarabine and/or allogenic HSCs transplantation. Patients within the favorable and intermediated risk groups often receive intensive chemotherapy, but unfortunately the risk of relapse still remains high and patients within the adverse risk group has often no advantage of being treated with intensive chemotherapy. Thus, this group of patients and patients within intermediate risk groups are also offered allogenic HSCs transplantation (25). It should be mentioned that the choice of treatment also depends on other factors, such as the patient age and performance status (28). One group of AML patients differs from all other AML subtypes, when it comes to treating these patients, namely the subtype M3 (Table 1), patients with APL. The standard care consists of treatment with vitamin A, all-trans retinoic acid combined with arsenic trioxide, and this chemo-free therapy often leads to high remission rate, hence high overall survival (38).

4.1.1 New approach of AML treatments

A new era within the AML treatment began in 2017, as an improved understanding of some of the underlying mechanisms behind AML pathogenesis has been reached. Before 2017, AML therapy had remained largely unchanged for decades (22). For the purpose of improving AML prognosis a broad spectrum of novel targeting agents has been developed. Drugs, such as Midostaurin, Gemtuzumab ozogamicin (GO), and Enasidenib were recently FDA approved for treatment of AML but is only focused towards specific subtypes of AML (26,39). For instance, Midostaurin, a multi kinase inhibitor, is able to target the oncogene *FLT3*. It was approved in combination with 7+3 treatment to patients harboring a FLT3-mutation. A study published in *The New England Journal of Medicine* demonstrated, that by combining Midostaurin to standard chemotherapeutic drugs the overall survival was increased. Newly diagnosed patients with *FLT3* mutation within the age of 18-59 was treated with either Midostaurin plus chemotherapy or only chemotherapy. The 4-year overall survival rate for patients treated with Midostaurin plus chemotherapy was 51.4% compared to the control group where

it was 44.3% (40). GO, an anti-CD33 antibody conjugated with the DNA toxin calicheamicin, was originally approved back in 2000, and was one of the first steps towards more personalized cancer target therapies. The drug was withdrawn due to questionable efficacy as no survival benefit was observed compared to standard therapy. With adjustments regarding efficacy, GO was reapproved in 2017 and is now utilized in the treatment of newly diagnosed adults with $CD33^+$ AML (26). Venetoclax is another recently FDA approved drug in treatment of hematological malignancies. It was first approved to treat chronic lymphocytic leukemia, and later approved in combination with azacitidine or decitabine or low-dose cytarabine to treat AML (41). Venetoclax is an orally bioavailable, small molecule inhibitor able to target the anti-apoptotic protein BCL-2, allowing for apoptosis. This drug is used for treatment of newly diagnosed AML patients older than 75 years and/or patients whom does not fit standard chemotherapy (42).

1.5 Aim of the present study

The overall objective in the present thesis is to establish new methods for identifying LSCs and to explore screens for chemicals that target LSCs in AML. To do this, first and foremost, a lentivirus is produced containing the vector pMIN-ERG+85, followed by an investigation on whether it is possible to transduce the AML cell lines, Kasumi-1, KG-1, and MOLM-13, with the lentivirus containing the pMIN-ERG+85 vector. The vector contains a constitutive green fluorescent protein (GFP) reporter gene and a blue fluorescent protein (BFP) reporter gene under the ERG+85 enhancer promoter. This reporter gene detects the endogenous ERG expression within the cells, which has been found to correlate with stemness in AML cells (35). Secondly, assuming successful transduction, cells positive for infection will be identified by GFP-expression, cells will then be sorted in order to only investigate GFP positive cells by the use of fluorescence activated cell sorting (FACS). Thirdly, the sorted populations will be long term cultured and investigated by flow cytometry in order to examine the GFP and BFP expression. Finally, the GFP positive populations will be tested by drug sensitivity with different agents. By using the BFP as a readout, this could give direct indications on agents that specifically target the LSC-population. Therefore, the hypothesis to be tested is that expression of BFP under the ERG+85 enhancer promoter in transduced AML cell lines would enable isolation of LSC-populations and thereby allowing for investigation of the response of LSCs to different chemotherapeutic agents.

2. Materials and Methods

The following section describes the methods performed in order to achieve the aim of the present thesis. An experimental timeline can be seen in Figure 3.

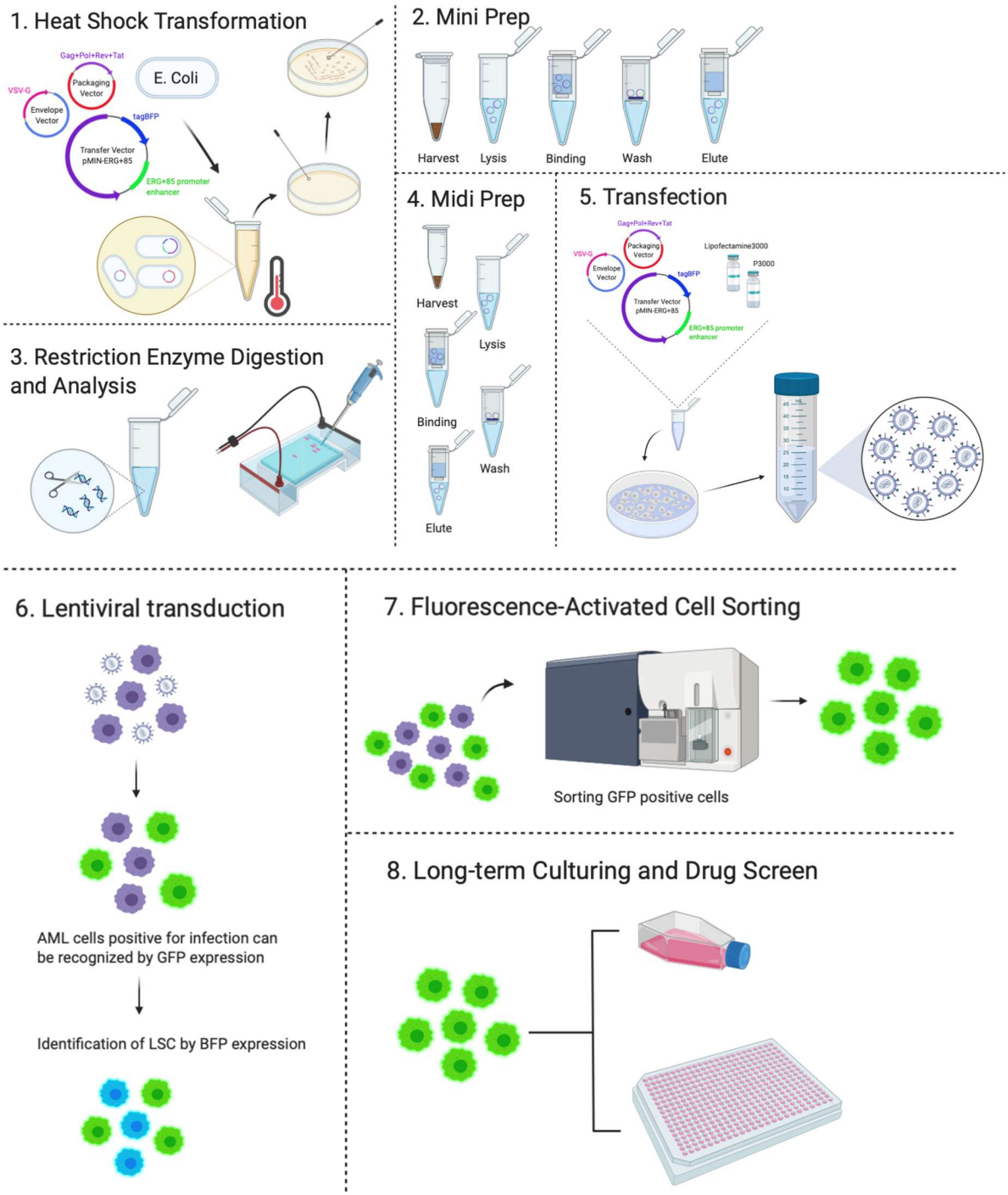

Figure 3. Overview of experimental timeline carried out in the present thesis in order to achieve the aim.

2.1 Plasmid extraction

The plasmids (Figure 4) received on filter paper were cut out by a sterile razor blade and immersed in Tris-EDTA buffer (pH=8.0) (Sigma, Cat. no.: 93283) for 10 min at room temperature. Subsequent to plasmid extraction, DNA concentrations were measured at a wavelength of 260 nm, and the purity of DNA were determined with a ratio of 260/280 nm using a spectrophotometer (NANODROP 2000c, Thermo Scientific). An overview of the plasmids can be seen in Figure 4. Transfer plasmids (plasmid A and B) were kindly provided by Dr. Milyavsky, Tel Aviv University, Israel. Packaging and envelope plasmids (plasmid C and D) were kindly provided by Dr. Daria Bulanova, FIMM, University of Helsinki, Finland. For a more comprehensive insight in packaging and envelope plasmids, see Appendix I.

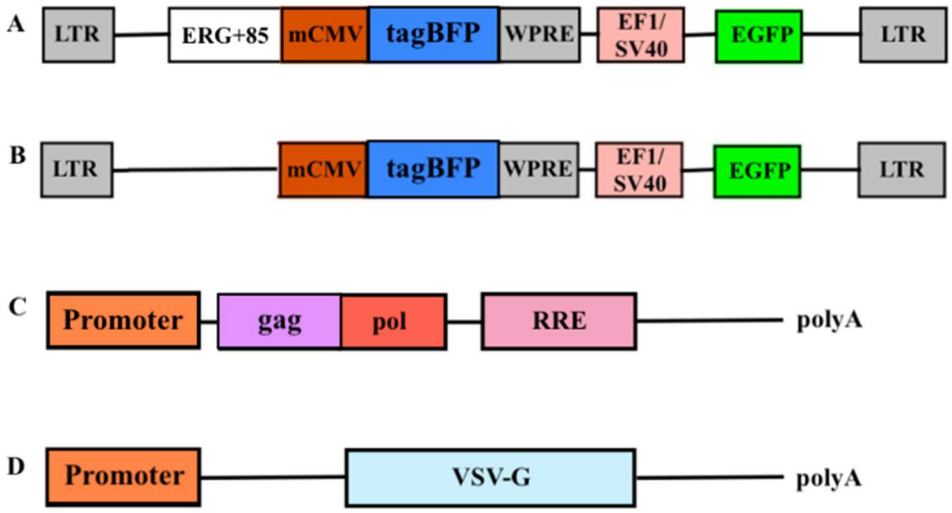

Figure 4. Structure of plasmids. A is plasmid pMIN-ERG+85, containing the ERG+85 enhancer promoter region. B is the pMIN backbone, used as a control. These are modified from (35)*. Plasmid C, pCMV dR8.91 used as a packaging plasmid, and D, pMD2.G used as envelope plasmid, respectively.*

2.2 Preparation of LB media and agar plates

To ensure optimal conditions for microbiological culturing and growth, lysogeny broth (LB) medium and agar petri dishes were prepared. In Table 3 there is an overview of the components.

Table 3. Components of LB media and agar media.

	LB medium	**Agar medium**
Bacto tryptone (Gibco, Cat. no.: 211705)	5 g	5 g

Yeast extract (Gibco, Cat. no.: 211929)	2.5 g	2.5 g
NaCl	5 g	5 g
Agar (Sigma, Cat. no.: 05040-100G)	-	7.5 g
dH_20	500 ml	500 ml

The components were mixed together followed by an autoclaving at 121° C under 20 psi for 30 min. The agar medium was cooled to a temperature between 40-60°C before adding ampicillin (Gibco, Cat. no.: 11593027) to a final concentration of 100 µg/ml. The agar medium was then poured into 100x15 mm petri dishes (Corning, Cat. no.: 07-202-011). The dishes were left to dry at room temperature later stored a 4° C. LB medium was stored at room temperature until further handling.

2.3 Heat shock transformation and mini prep

In order to transform competent *Escherichia coli* XL1-blue (Agilent, Cat. no: 200249) cells with plasmids shown in Figure 4, the manufactory protocol was followed (43). β-mercaptoethanol was added to the competent cells and subsequently incubated on ice for 10 min while gently being mixed every 2 min. Afterwards, plasmids were added to competent cells and incubated on ice for 30 min, followed by heat shock transformation at 42°C for 45 s and incubated on ice for 2 min. Preheated S.O.C. medium (Invitrogen, Cat. no.: 15544-034) was added to the cells and the mixture was transferred to Falcon round bottom tubes (Corning Cat. no.: 352059). The transformed XL1-blue cells in S.O.C. media were then incubated at 37°C for 1 h in Forma Orbital Shaker (Thermo Scientific) at 200 rounds per minute (rpm) and subsequently plated on agar dishes containing ampicillin. The dishes were incubated overnight at 37°C. After overnight incubation, bacteria colonies were selected and added to fresh LB media, containing 100 µg/ml ampicillin, in Falcon round bottom tubes and incubated overnight at 37°C in the aforementioned incubator at 200 rpm. ¾ of the overnight cultures were isolated by using Qiagen QIAprep Spin Mini prep Kit in order to retrieve plasmid DNA. Here, the manufacturer's protocol for Mini prep (44) was followed, and DNA concentrations were measured using a spectrophotometer (NANODROP 2000c, Thermo Scientific). Purified plasmids were aliquoted and

stored in -20°C and the remaining ¼ bacteria culture was stored at 4°C and to be used for the upscaling bacteria culture, described in section *2.5 Upscaling bacteria culture and midi prep*.

2.4 Restriction enzyme digestion

By ensuring integrity of the purified plasmids, a restriction enzyme analysis was carried out. First, mini prep purified samples were thawed on ice, followed by mixing with CutSmart Buffer 10X (New England BioLabs, Cat. no.: B7204S), restriction enzymes: EcoRI (New England BioLabs, Cat. no.: R0101L) and/or BamHI (New England BioLabs, Cat. no.: R0136L) and dH_20. The mixture was then incubated for 1 h at 37°C. The digested samples were loaded with 10X Loading buffer and SYBR™ Safe DNA Gel Stain (Invitrogen, Cat. no.: S33102) on a 1% agarose gel in 0.5% TAE buffer placed in a horizontal electrophoresis system (BIO-RAD) according to setup in Table 4. The gel was run at 90 V for 30 min. MassRuler DNA Ladder (Thermo Scientific, Cat. no.: SM0403) was utilized to quantify band size of DNA fragments. To visualize where band sizes were located a Molecular Imager XR+ (BIO-RAD) was utilized.

Table 4. Overview of well setup for restriction enzyme digestion.

Well	**1**	**2**	**3**	**4**	**5**	**6**	**7**	**8**	**9**
RE	-	EcoRI		BamHI		EcoRI		EcoRI + BamHI	
Plasmid	Ladder	pMIN-ERG+85		pMIN		pMD2.G		pCMV dR8.91	

2.5 Upscaling bacteria culture and midi prep

To purify larger quantities of plasmids, an upscaling of the bacteria culture was carried out. Briefly, the remaining overnight culture from *2.3 Heat shock transformation and mini prep* was plated on agar dishes with ampicillin and incubated overnight at 37°C. The following day, one colony from each plate were selected and added LB media containing 100 µg/ml ampicillin, transferred to Falcon round bottom tubes, and incubated at 37°C for 6 h in a Forma Orbital Shaker at 200 rpm. After incubation, the day culture was diluted in 1:1000 in LB media containing 100 µg/ml ampicillin, transferred to Erlenmeyer flasks, and incubated overnight at the same settings. Then plasmid DNA was isolated from the bacteria culture using Qiagen QIAprep Spin Midi prep Kit according to the manufacturer's instructions (44). DNA concentrations

were measured using a spectrophotometer (NANODROP 2000c, Thermo Scientific), and samples were aliquoted and stored in -20°C until further handling.

2.6 Cell line culture

Human embryonic kidney (HEK) 293T, Kasumi-1 and MOLM-13 cells were kindly provided from a colleague in the laboratory. KG-1 cells were obtained from DSMZ (Leibniz Institute). HEK 293T cells were cultured in high-glucose Dulbecco's Modified Eagle Medium (DMEM) (Gibco, Cat. no.: 11995065) supplemented with 10% heat inactivated fetal bovine serum (FBS) (GE Healthcare Hyclone, Cat. no.: SV30.160.03) and 1% penicillin/streptomycin (pen-strep) (Sigma, Cat.: P0781). Kasumi-1, KG-1 and MOLM-13 cells were cultured in high-glucose Roswell Park Memorial Institute (RPMI) 1640 medium (Gibco, Cat. no.: 61870036) supplemented 20% heat inactivated FBS and 1% pen-strep. Cells were incubated under standard cell culture conditions at 37 °C in humidified atmosphere containing 5% CO_2 and 20% O_2. Splitting of cells occurred when the level of confluence was 80-90%. Culture media were change every three day, unless other is stated.

2.7 Transfection of HEK 293T cells and production of lentivirus

All work with lentivirus was performed in GMO2 class laboratory and carried out in accordance to the safety guidelines for handling of genetically modified organisms.

For lentiviral production, HEK cells were transfected using Lipofectamine3000 with either pMIN-ERG+85 or pMIN along with packaging and envelope plasmids pCMV dR8.91 and pMD2.G in order to produce and secrete lentivirus to the supernatant. The manufacturer's guidelines for lentiviral production (Invitrogen) were followed, however with slightly modifications (45). Shortly, HEK 293T cells were seeded in a concentration of $1.25x10^6$ in a 6-well plate (Corning Costar, Cat. no.: 3516) in 2.0 ml/well of Opti-MEM (Gibco, Cat. no.: 11058021) with 5% heat inactivated FBS followed by an overnight incubation at 37°C. The following day, half of the Opti-MEM medium were replaced with a mixture of fresh Opti-MEM, 0.7 µg of plasmid pMD2.G, 3.3 µg of plasmid pCMV dR8.91, 4 µg of either pMIN-ERG+85 or pMIN, 6 µl of the enhancer reagent of P3000 (Thermo Fisher, Cat. no.: L3000001) and 7 µl of the transfection reagent Lipofectamine3000 (Thermo Fisher, Cat. no.: L3000015). Cells were incubated in the mixture media for 6 h, followed by a media change with fresh Opti-MEM and

incubated overnight at 37°C. 24 h post transfection, the first batch of the viral supernatant was harvested and replaced with fresh media and incubated overnight at 37°C. Second batch of the viral supernatant was collected approximately 52 h post transfection and pooled together with the first batch. The viral supernatant was centrifuged at 2.000 rpm, pellet was discarded, and the supernatant were filtered using a 0.45 µm pore filter to remove any remaining cellular debris. Viral supernatant was aliquoted in cryovials and stored in -80°C until further handling.

2.8 Pilot transduction of HEK 293T cells

The objective was to test whether the lentivirus produced in *2.7 Transfection of HEK 293T cells and production of lentivirus* worked efficiently and was able to infect cultured cells, in this case HEK 293T cells. Firstly, cells were seeded in a 24-well plate (Nunc, Cat. no.: 142475) with a concentration of $1.25x10^5$ in 1.0 ml/well culture media and incubated overnight at 37°C. After allowing cell adherence 100 µl of either pMIN-ERG+85 or pMIN lentiviral supernatant were added. In half of the samples 8 µg/ml polybrene (Sigma, Cat. no.: TR1003G) was added as a transducing agent to test whether a difference within the transduction efficiency appeared. Cells were centrifuged at 2.000 rpm for 30 min and incubated overnight. Medium was changed the following day, and again on day 4. On day 7, cells were trypsinized, washed with phosphate buffered saline (PBS) and transferred to a 96-well plate (Nunc, Cat. no.: 621262) in order to investigate transduction by flow cytometry using IntelliCyt® iQue Screener PLUS. The flow cytometry data was further analyzed using FCS Express 7 Research.

2.9 Titration of lentivirus by GFP expression in Kasumi-1, KG-1 and MOLM-13 cells

The objective was to determine the viral titer in order to calculate transducing unit (TU) pr. ml. The TU/ml can further be used to assess the amount of virus supernatant needed, when a multiplicity of infection (MOI) of 10 is desired.

All three AML cell lines were transduced in a 96-well, V-bottom plate (Thermo Fisher, Cat. no.: 249940) with the concentration of $7x10^3$ cells in 100 µl culture media supplemented with 8 µg/ml polybrene (Sigma, Cat. no.: TR1003G) pr. well. In order to transduce the cells with different concentrations of the virus, serial dilutions were mixed according to the setup in Appendix II. After preparing different concentrations of the virus and adding them to the cells, they were centrifuged at 2.000 rpm for 30 min at room temperature and incubated overnight at

37ºC. Medium were changed the following day, and again on day 4. On day 7 post transduction, cells were washed with PBS followed by analyzing the percentage of GFP positive cells by flow cytometry using IntelliCyt® iQue Screener PLUS. Data obtained from the flow analysis was further analyzed using FSC Express 7. Analysis of the titrations enabled the calculation of TU/ml, which were utilized for further transduction of Kasumi-1 and MOLM-13 cells, but not KG-1 cells.

2.10 Lentiviral transduction of Kasumi-1 and MOLM-13 cells

The purpose was to transduce Kasumi-1 and MOLM-13 cells with both pMIN-ERG+85 and pMIN with a MOI at 10. Briefly, Kasumi-1 cells were transduced in a 24-well plate (Corning, Cat. no.: CLS3473) with the concentration of $3x10^4$ cells in 1.0 ml culture media supplemented with 8 µg/ml polybrene (Sigma, Cat. no.: TR1003G) and the appropriate amount of viral supernatant from either pMIN-ERG+85 or pMIN. MOLM-13 cells were also transduced in a 24-well plate but with the concentration of $1.5x10^4$ cells in 1 ml culture media supplemented with 8 µg/ml polybrene (Sigma, Cat. no.: TR1003G) and the correct volume of viral supernatant. After addition of the virus, cells were centrifuged at 2.000 rpm for 30 min at room temperature and incubated overnight at 37ºC. Medium were changed the following day, and onwards every three days. On day 1 post transduction, cells were investigated by GFP expression. The images were captured using the Leica DMI6000 B fluorescent microscope, in order to verify successful transduction. On day 7 and 28 post transduction, cells were washed with PBS followed by analyzing the GFP and BFP expression by flow cytometry using IntelliCyt® iQue Screener PLUS. The flow cytometry data was further analyzed utilizing the program FCS Express 7 Research.

2.11 FACS of ERG+85 reporter expressed in Kasumi-1 cells and MOLM-13 cells

In order to investigate only cells positive for infection, the transduced Kasumi-1 and MOLM-13 cells were sorted by FACS. Cells were washed with PBS/0.5%BSA followed by staining the cells with DRAQ7 (BioLegend, Cat. no.: 424001), in the concentration of 1:100, to distinguish between viable and dead cells, as DRAQ7 stains the nuclei in dead cells. Cells were incubated in the dark with DRAQ7 for 30 min and subsequently washed. Cells were then placed on ice and transferred to the FACS Facility, where cells were sorted with help from the facility

staff using a FACS Aria III. After sorting the cells, they were washed and culture medium were added, and subsequently cultured in a 24 well plate (Corning, Cat. no.: CLS3473) and placed in the incubator until further handling.

2.12 Cell growth and count

In order to follow the growth of lentivirally transduced cells after they were sorted by FACS, cells were stained with trypan blue (Invitrogen, Cat. no.: T10282) in the concentration of 1:1. The mixture was added to a cell counting chamber from same manufacturer and automatic counted using the Countess™ Automated Cell Counter from Invitrogen. By staining the cells with trypan blue, the automatic counter was able to distinguish between viable and dead cells, as the dead cells are stained with trypan blue.

3. Results

In the following section results from the study will be presented, starting with the assessment of plasmid concentration and validation of plasmid integrity by restriction enzymes analysis. This will be followed by a presentation of flow cytometry results from lentiviral transduction experiments, which includes the virus titration setup and gating strategy utilized for the analysis. Moreover, results from FACS on transduced cell lines will be presented, followed by growth assessments on lentivirally transduced, FACS sorted AML cell lines. Data presented from flow cytometry and growth assessments are results of single experiments.

3.1 Propagation of transfer and packaging plasmids

The plasmids to be utilized for lentiviral production pMIN-ERG+85, pMIN, pMD2.G and pCMV dR8.91 were transformed into *Escherichia coli* XL1-blue competent bacteria cells and transformed cells were then cultured and expanded. The bacteria were handled as described in the method section *2.3 Heat shock transformation and mini prep.* Plasmid DNA was purified with mini prep kit and DNA concentrations were assessed by spectrometry on a Nanodrop 2000c instrument. After the concentration of mini prep purified samples were measured, and plasmid integrity ensured by restriction enzyme analysis (See section *3.2 Plasmid verification by restriction enzyme analysis*), an upscaling of bacteria culture was performed, and plasmid DNA was purified using midi prep. The plasmid concentrations obtained by midi prep purification (Table 5) proved sufficient to be used for lentivirus production (See section *3.3 Validation of lentiviral production*).

Table 5. Overview of plasmid concentration after extraction, mini prep, and midi prep, respectively. All concentrations were measured as ng/µl on spectrophotometer (NANODROP 2000c, Thermo Scientific).

	pMIN-ERG+85	**pMIN**	**pMD2.G**	**pCMV dR8.91**
Extraction	31.5	68.8	4.3	5.1
Mini Prep	204.3	169.0	102.8	73.1
Midi Prep	1064.1	1090.4	529.4	453.6

3.2 Plasmid verification by restriction enzyme analysis

Mini prep purified samples were investigated by restriction enzyme analysis to ensure the integrity of the plasmids. The restriction enzymes used to cut the plasmids were EcoRI and BamHI, as described in the method section (*2.4 Restriction enzyme digestion*). From plasmid map investigation, shown in Appendix III, digested fragments were expected to have band sizes of 1370 and 7923 base pair (bp) for plasmid pMIN-ERG+85 when using restriction enzyme EcoRI. To cut plasmid pMIN, the restriction enzyme BamHI was used and the length of the digested plasmid was expected to 8837 bp. For plasmid pMD2.G the band size fragments were expected to be 1668 and 4154 bp when using restriction enzyme EcoRI. To cut plasmid pCMV dR8.91 both restriction enzymes, EcoRI and BamHI, were used and fragments sizes were expected to be 1273 and 10877 bp. By observing the fragment pattern of the digested plasmids in Figure 5, it can be seen that the bands closely resemble the expected sizes. One exception is pMIN, where extra bands are evident when only one band would be expected from complete digest. This was considered to be a result of incomplete digestion and the plasmid was therefore nevertheless decided to be continued for bacteria upscaling.

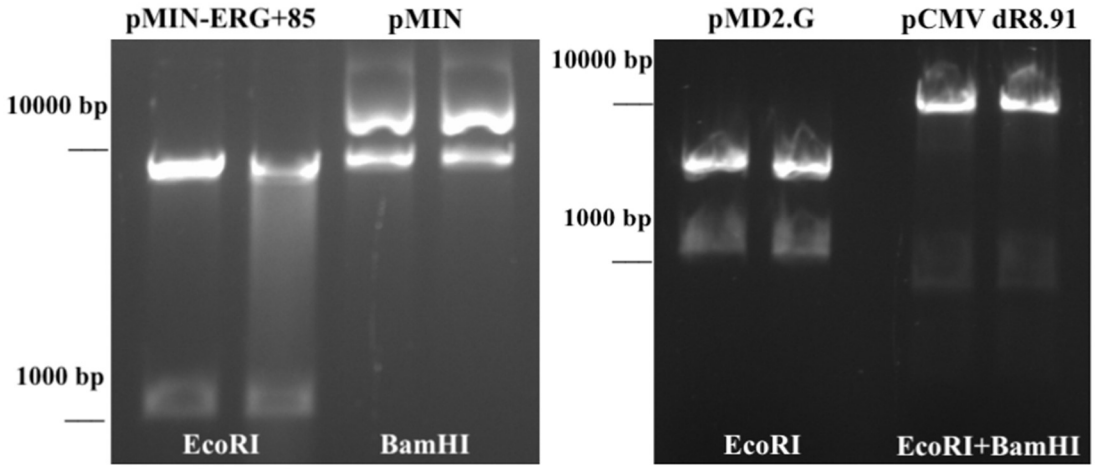

Figure 5. Image of restriction enzyme digestion. The length of digested bands closely resembles the expected sizes from the restriction digestion with the only exception of plasmid pMIN. The fragment sizes were expected to be 1370 and 7923 base pair (bp) for pMIN-ERG+85 when using restriction enzyme EcoRI. Digested plasmid pMIN were expected to have length of 8837 bp when using restriction enzyme BamHI. For digested plasmid pMD2.G the band size fragments were expected to be 1668 and 4154 bp, when using restriction enzyme EcoRI. Finally, digested plasmid pCMV dR8.91 was expected to be 1273 and 10877 bp, when using both restriction enzymes. The wells were set as duplicates.

3.3 Validation of lentiviral production

To produce lentivirus containing either plasmid pMIN-ERG+85 or pMIN, HEK 293T cells were transfected by means of Lipofectamin3000, plasmid pMD2.G and pCMV dR8.91 as described in method section (*2.7 Transfection of HEK 293T cells and production of lentivirus*). To validate if the produced lentivirus worked efficiently and were capable of infection HEK 293T, cells were subsequently transduced with the produced lentivirus.

3.3.1 Gating strategy for flow cytometry

A gating strategy was established to assess the percentage of cells that had been transduced with the lentivirus, as determined by expression of GFP in a flow cytometer. Live cells were run through the flow cytometer, and forward scatter (FSC), side scatter (SSC) and green fluorescence were monitored. To analyze the percentage of GFP expressing cells, the detected events from the flow cytometer were first visualized in an SSC-H/FSC-H density plot where cells were separated from debris, seen in Figure 6, panel A. Additionally, an FSC-H/FSC-A density plot was utilized to gate the singlets, seen in panel B. To distinguish between GFP expressing cells and non-GFP expressing cells, a negative control was included, where no virus supernatant was added, allowing for setting a gate on GFP expressing cells that would include 0.00% of the negative control cells as seen panel C. GFP would be expected to be excited by a 488nm laser and therefore detected in the Blue laser channel (530/30). The same gating strategy was used during analysis for all flow cytometry data in this study.

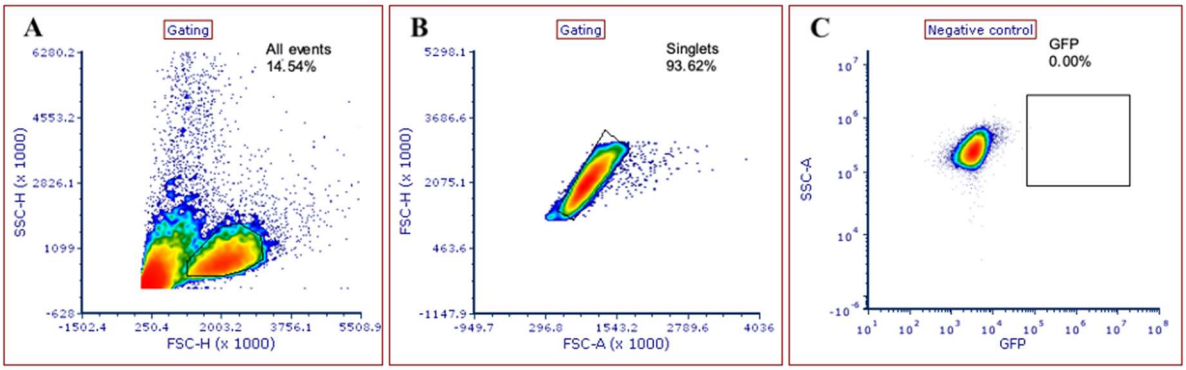

Figure 6. An example of the gating strategy performed throughout the project. Panel A, all events of interest were gated using an SSC-H/FSC-H density plot. Panel B, singlets were gated using an FSC-H/FSC-A density plot. In panel C, the GFP gate were set on a negative control of cells not transduced with virus.

3.3.2 Assessment of transduction in HEK 293T cells

To validate successful packaging and transduction efficiency of the produced lentivirus, HEK 293T cells were infected. It is evident that the produced lentiviruses were able to infect HEK 293T cells, as the cells are partially expressing GFP, which indicates infection as seen in Figure 7. Additionally, the transduction agent, polybrene, was added to test whether an effect could be observed on the transduction efficiency. When comparing the population of GFP expressing cells between samples with (A/C) and without polybrene (B/D), it shows a distinct increase in transduction when cells are transduced in the presence of polybrene. Thus, it has been successfully shown that both viruses are able to infect cells, and further, that the transduction efficiency was increased by the addition of polybrene, which will therefore be used for all further transduction experiments.

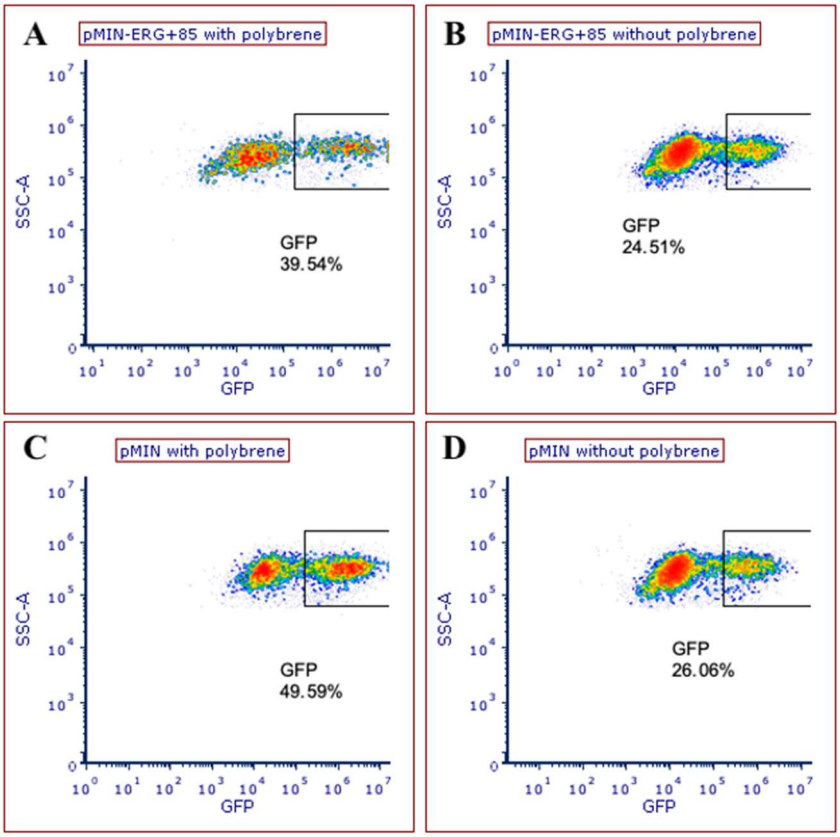

Figure 7. Transduction with lentivirus in HEK 293T cells. In panel A, cells were infected with the lentivirus containing pMIN-ERG+85 using polybrene and panel B shows infection without polybrene. The same principal occurs in panels C and D, infected with lentivirus containing pMIN.

3.4 Assessment of transducing units by titration of lentivirus

As described in the method section *2.9 Titration of lentivirus by GFP expression in Kasumi-1, KG-1 and MOLM-13 cells*, the viral titer must be determined in order to calculate the amount of viral supernatant needed when a MOI of 10 is desired, which refers to the number of infected viral particles pr. cells. The three AML cell lines, Kasumi-1, KG-1, and MOLM-13 were used to determine TU by titration of the lentivirus vector containing pMIN-ERG+85. Titration experiments for the lentiviral vector containing pMIN can be seen in Appendix IV.

3.4.1 Titration of lentivirus by GFP

As earlier mentioned, the expression of GFP in transduced cells is an indication of successful infection, hence the higher percentage of GFP expressing cells, the more efficient transduction. In order to determine the TU, each of the AML cell lines were transduced with a serial titration of the virus supernatant.

For the cell lines, Kasumi-1 and MOLM-13, flow cytometry analysis showed that the cells were infected successfully with the lentivirus containing pMIN-ERG+85 (Figure 8 and 9). Moreover, it can be observed that the percentage of GFP expressing cells are decreasing as a function of the virus concentration. Conversely, the AML cell line KG-1 presented with a low infection rate demonstrating very little transduction as observed by the low percentage of GFP for all four dilutions with the lentivirus containing pMIN-ERG+85 (Figure 10).

Figure 8 shows the titration data obtained by pMIN-ERG+85 transduction of Kasumi-1 cells. In panel A, 36.07% of the cells are infected with the lentivirus, followed by 13.48% of the cells in panel B, 0.64% in panel C and lastly, 0.08% in panel D.

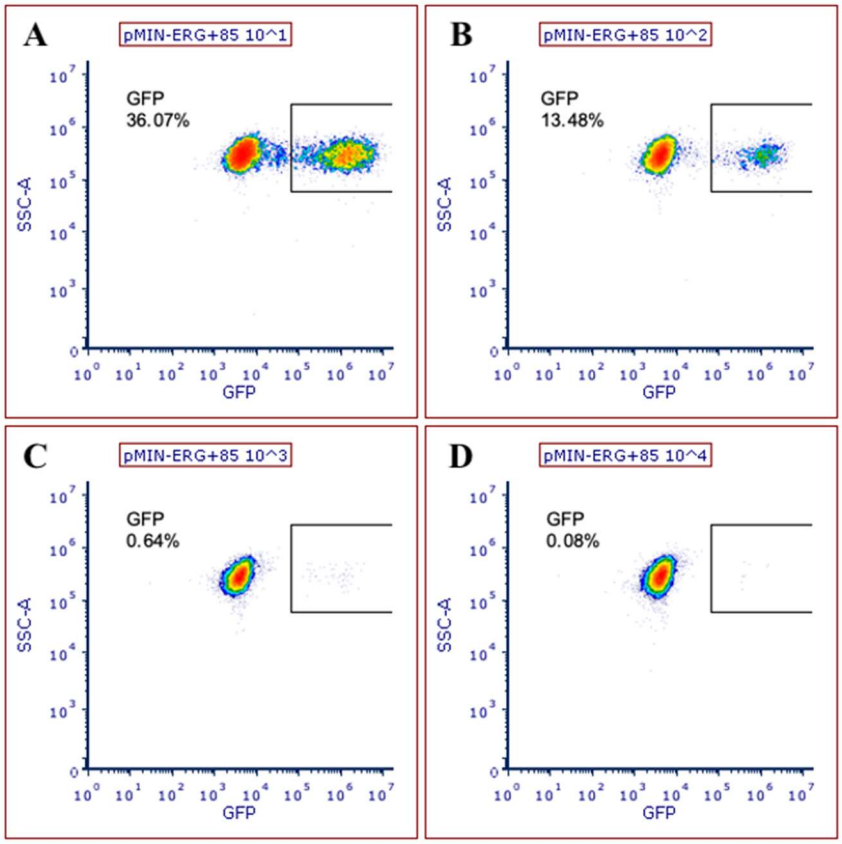

Figure 8. Titration of lentivirus by GFP expression in Kasumi-1 cells. Panel A, has the highest virus concentration, followed by B, C and D.

Flow cytometry results from titration experiment by GFP expression in MOLM-13 cells are presented in Figure 9. Starting with panel A, 15.10% of the cells are expressing GFP, followed by a descending GFP expression in panel B with 3.95%, 0.24% in panel C, and no cells are expression GFP in panel D, hence no infection.

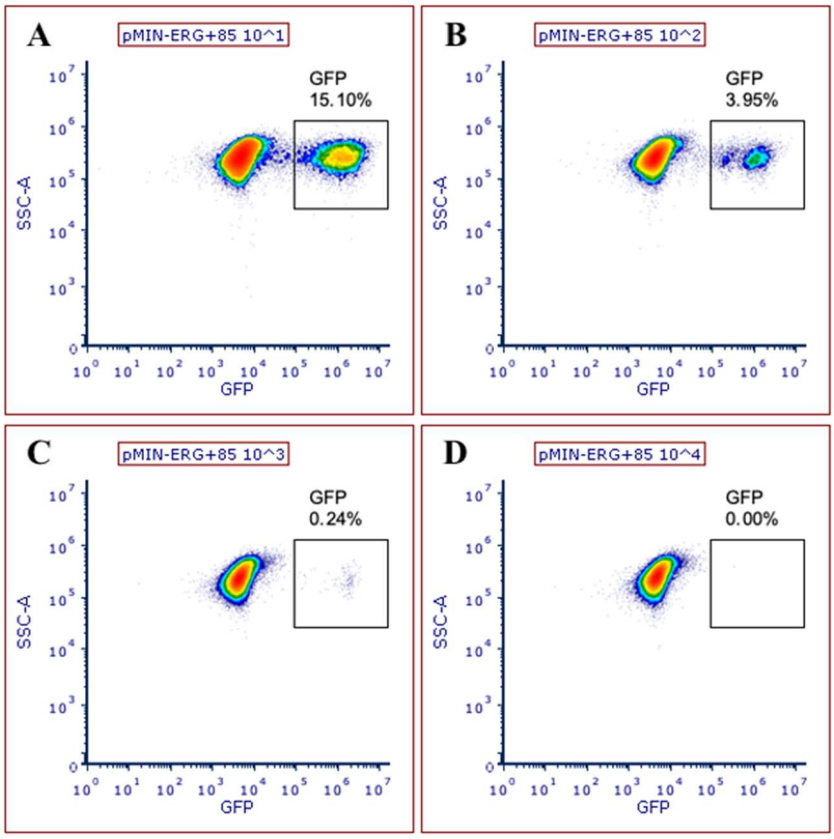

Figure 9. Titration of lentivirus by GFP expression in MOLM-13 cells. The highest virus concentration is used in panel A, and are descending when looking at panels B, C, and D.

Lastly, results from titration experiment of lentivirus by GFP expression in KG-1 cells appears in Figure 10. In panel A, 0.37% of the KG-1 cells are expressing GFP, followed by 0.09% in panel B, 0.02% in panel C and 0.01% GFP expressing cells were present in panel D.

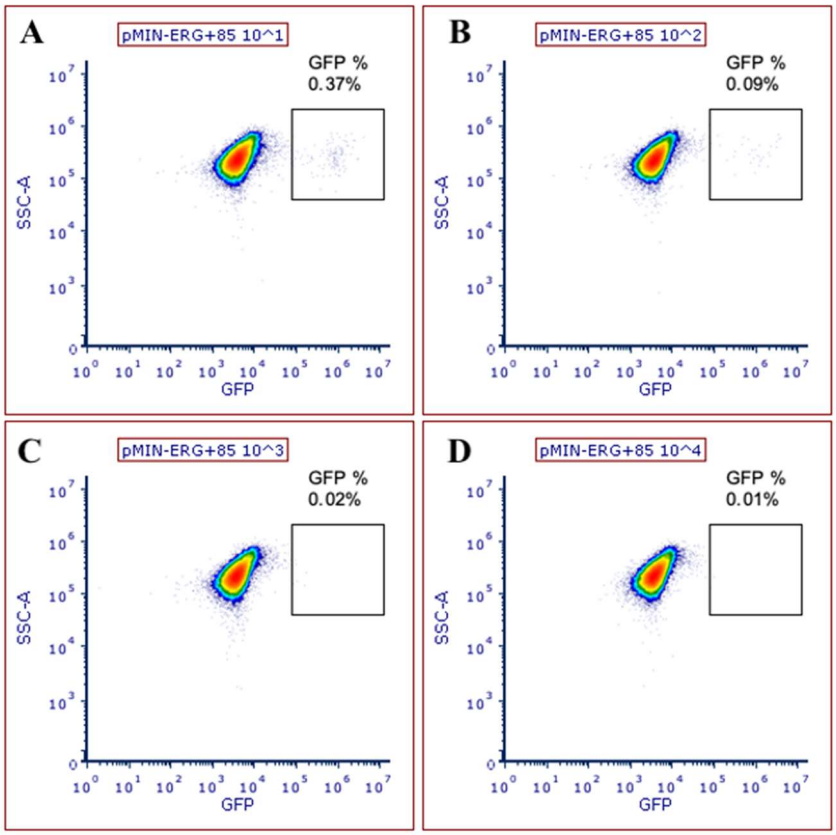

Figure 10. Titration of lentivirus by GFP expression in KG-1 cells. The highest virus concentration is seen in panel A, and are declining when looking at panels B, C, and D.

After analysis of the different cell lines by ability to be transduced as established by the GFP expression, it was decided that Kasumi-1 and MOLM-13 were more optimal to be used for further experiments. This was determined by the poor infection rate of KG-1 with either pMIN-ERG+85 or pMIN virus. Following this decision TU for Kasumi-1 and MOLM-13 cells were calculated for either virus, and this knowledge along with the desired MOI were used for calculating the amount of virus supernatant to be used when transducing, as seen in Table 6. For a detailed insight of the TU calculations, see Appendix V.

Table 6. Summary of TU and MOI for Kasumi-1 and MOLM-13 cells, for both pMIN-ERG+85 and pMIN.

	Kasumi-1	MOLM-13
TU/ml	pMIN-ERG+85 = 9.38×10^5 TU/ml pMIN = 3.99×10^6 TU/ml	pMIN-ERG+85 = 1.057×10^5 TU/ml pMIN = 8.407×10^5 TU/ml
MOI at 10	pMIN-ERG+85 = 319 µl pMIN = 75.1 µl	pMIN-ERG+85 = 1410 µl pMIN = 178 µl

3.5 Assessment of transduced Kasumi-1 and MOLM-13 cells

One of the overall aims of this study was to isolate LSC population within AML cell lines. To do that, Kasumi-1 and MOLM-13 cells were infected with both pMIN-ERG+85 and pMIN lentiviral vectors. By investigating the GFP expression in lentivirally transduced cells with fluorescent microscopy it allows for confirming successful infection. Following investigating by flow cytometry it first allows for discriminating between infected and non-infected cells by GFP. Moreover, the BFP expression can be used to indicate transcriptional binding to the ERG+85 enhancer promoter, as the BFP reporter gene relates to the endogenous ERG expression within the cells, which is found to correlate with stemness within LSC. It should be mentioned that Kasumi-1 cells are expected to express the gene for ERG, whereas MOLM-13 cells are used, as they do not express the gene for ERG.

3.5.1 Fluorescent microscopy assessment

On day 1 post transduction, Kasumi-1 and MOLM-13 cells were investigated by GFP expression using fluorescent microscopy. As seen in Figure 11, Kasumi-1 cells are expressing GFP after transduction with the lentiviral vector containing either pMIN-ERG+85 or pMIN, indicating successful infection with a MOI of 10. No GFP expression was observed in the negative control, despite the presence of cells in the well as seen by Figure 11, panel A.

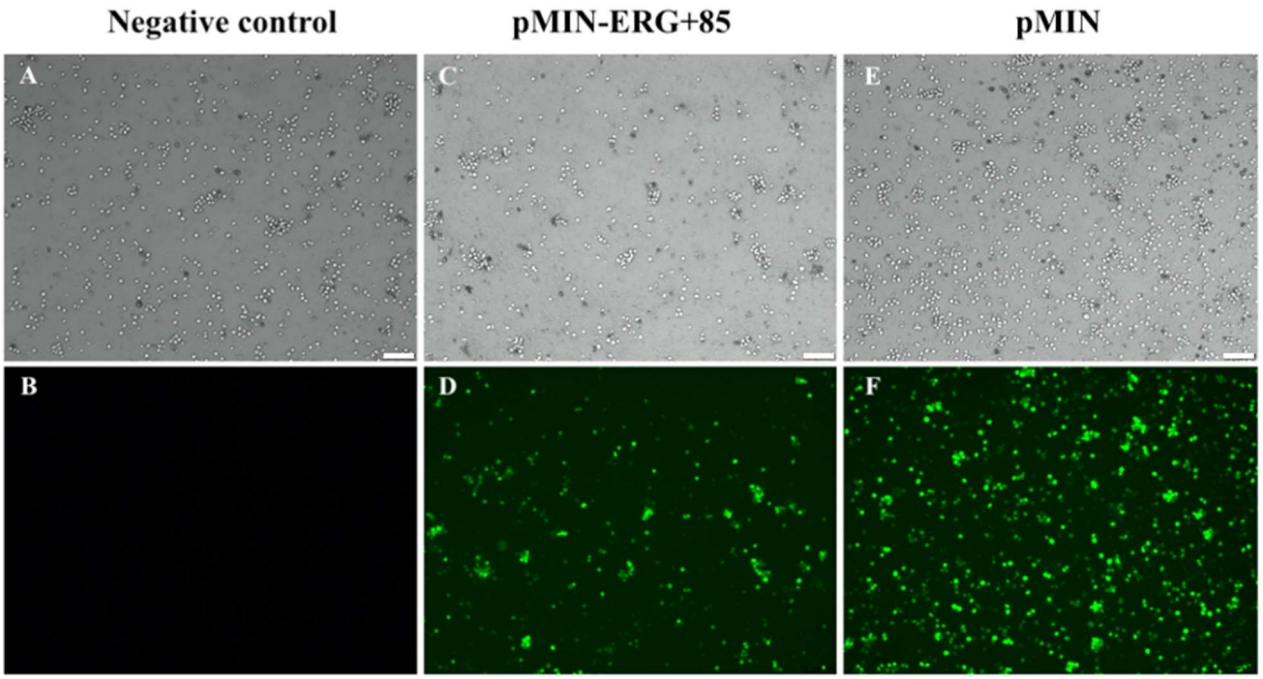

Figure 11. Images of the transduced Kasumi-1 cells on day 1 post transduction. The top panels show phase contrast images, while lower panels show the fluorescent images. Panels A and B are the negative controls, panels C and D represents cells transduced with the lentiviral vector containing pMIN-ERG+85, and finally in panels E and F cells are transduced with the lentiviral vector containing pMIN. Scales bars: 100 µm for all images.

Likewise, MOLM-13 cells were successfully transduced as seen by GFP expression after transduction with the lentiviral vector containing either pMIN-ERG+85 or pMIN. No GFP expression was present in the negative control, seen in Figure 12.

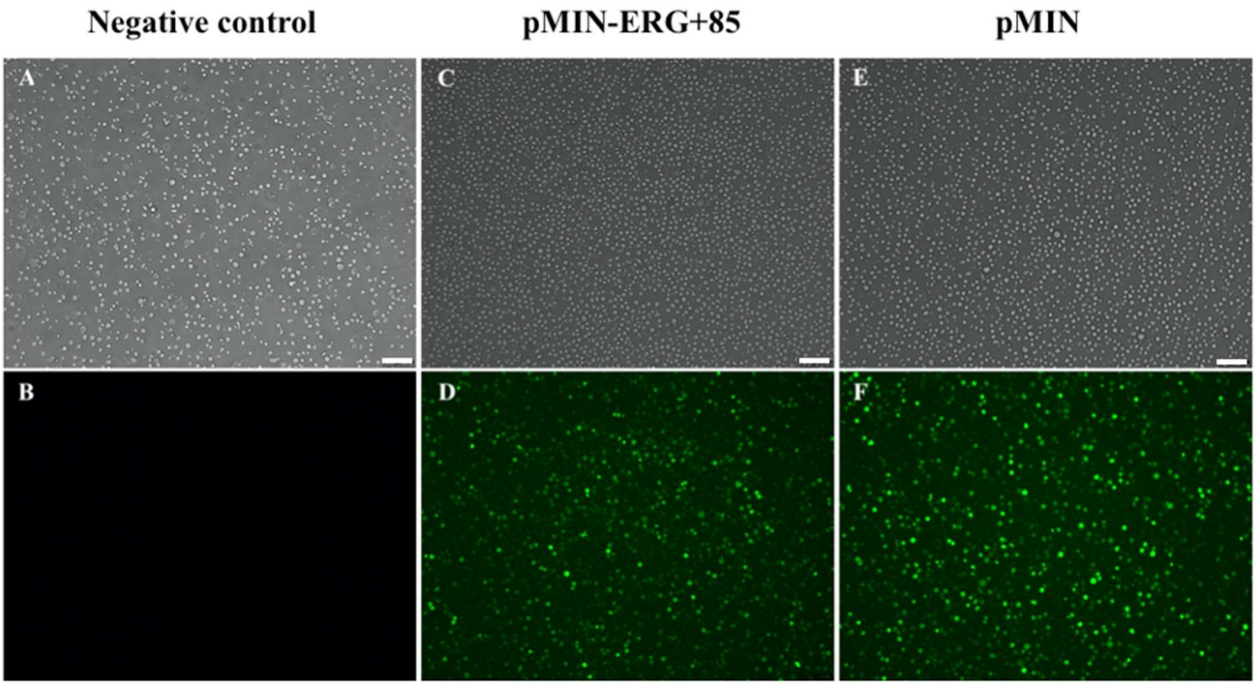

Figure 12. Images of the transduced MOLM-13 cells on day 1 post transduction. The top panels show phase contrast images, while lower panels show the fluorescent images. Panels A and B are the negative controls, panels C and D represents cells transduced with the lentiviral vector containing pMIN-ERG+85, and finally in panels E and F cells are transduced with the lentiviral vector containing pMIN. Scale bars: 100 µm for all images.

3.5.2 Flow cytometry analysis of transduced Kasumi-1 and MOLM-13 cells

The AML cell lines, Kasumi-1 and MOLM-13, were investigated by flow cytometry on day 7 post transduction to measure both GFP and BFP expression. BFP would be expected to be excited by a 405nm laser and therefore detected in the violet laser channel (445/45). By looking at the GFP expression on day 7 post transduction for Kasumi-1 cells transduced with the lentiviral vector containing pMIN-ERG+85, it could be seen that 75.99% of the cells were expressing GFP and further within the GFP positive population, 0.98% of the cells were expressing BFP. For cells transduced with the lentiviral vector containing pMIN 84.71% of the cells were expressing GFP and within the GFP positive population 59.86% of the cells were expressing BFP (Figure 13).

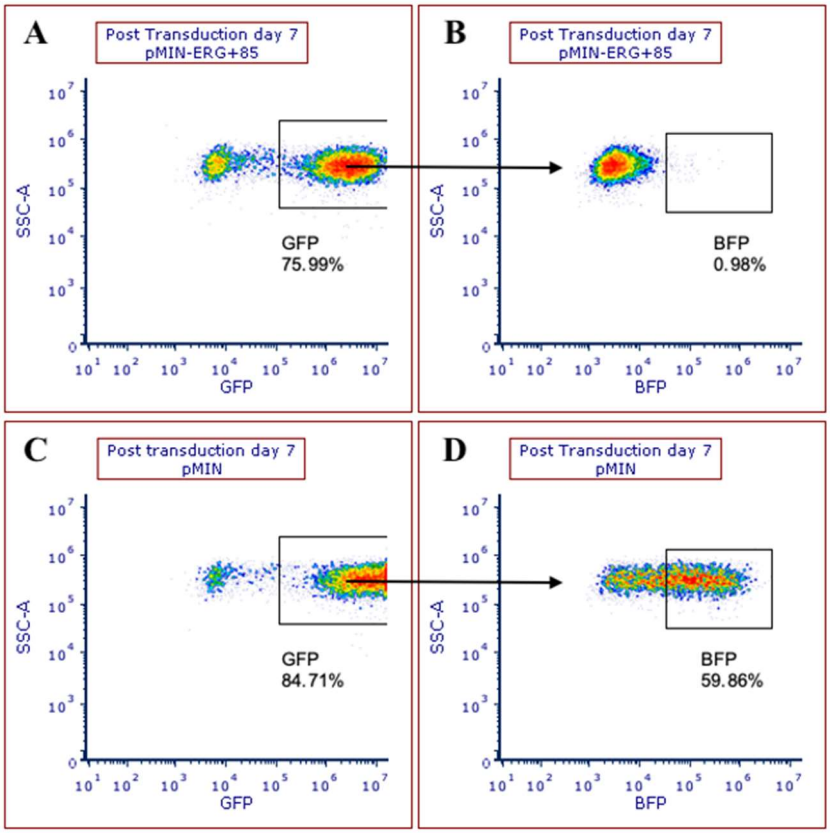

Figure 13. Flow cytometry analysis on day 7 post transduction for Kasumi-1 cells. In panels A and B, cells were transduced with the lentiviral vector containing pMIN-ERG+85, panel A shows the GFP

expression, while panel B shows the BFP expression within the GFP positive population. In panel C and D, Kasumi-1 cells were transduced with the lentiviral vector containing pMIN, showing GFP expression in panel C and BFP expression within the GFP positive population in panel D.

Analysis of MOLM-13 cells transduced with the lentiviral vector containing pMIN-ERG+85 7 days post transduction are expressing 54.17% GFP, whereas the BFP expression within the GFP positive population are 33.92%. For MOLM-13 cells transduced with the lentiviral vector containing pMIN, the GFP positive population was 65.39%, and the BFP expression within the GFP positive population is 59.13%, as seen in Figure 14.

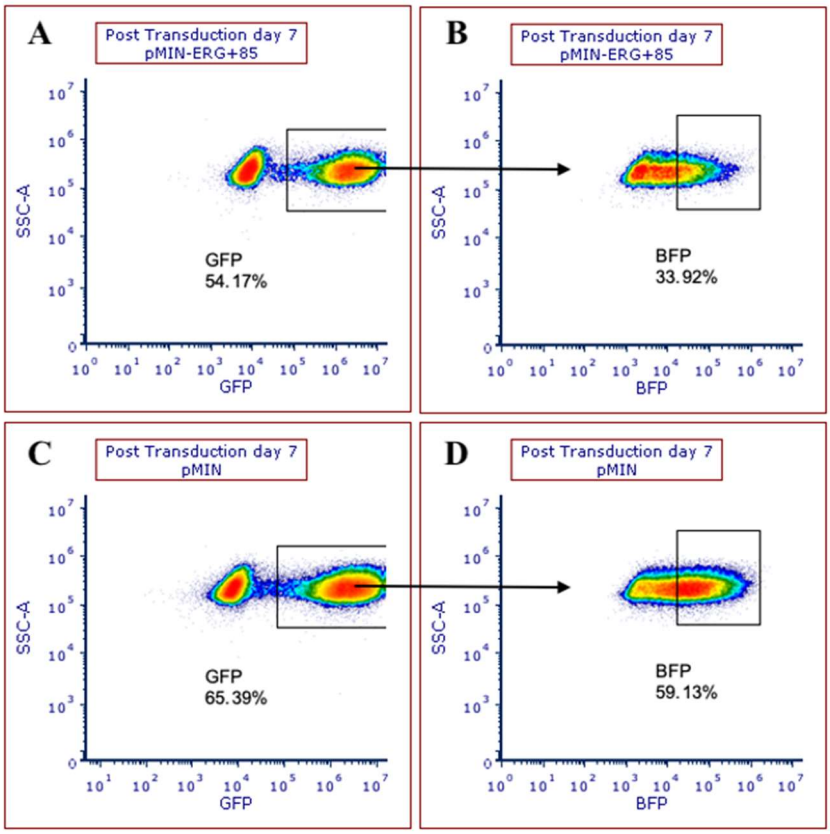

Figure 14. Flow cytometry analysis on day 7 post transduction for MOLM-13 cells. In panels A and B, cells were transduced with the lentiviral vector containing pMIN-ERG+85, panel A displaying GFP expression, whereas panel B are representing the BFP expression within the GFP positive population. In panels C and D, cells were transduced with the lentiviral vector containing pMIN, in panel C the GFP expression are presented, while the BFP expression within the GFP positive population can be seen in D, respectively.

Overall, investigations of transduced Kasumi-1 and MOLM-13 cells by both fluorescent microscopy and flow cytometry on day 1 and 7 post transduction, respectively, showed that the AML cell lines were successfully transduced with the lentiviral vector containing either pMIN-

ERG+85 or pMIN when using a MOI of 10. However, when looking into the BFP expression on day 7 post transduction, a higher BFP expression was observed in the control vector pMIN, compared to pMIN-ERG+85 for both AML cell lines. This was unexpected, as the pMIN does not contain the ERG+85 enhancer promoter but only the minimal cytomegalovirus (mCMV) promoter.

3.6 FACS of Kasumi-1 and MOLM-13 cells for investigation of BFP expression

The transduced AML cell lines, Kasumi-1 and MOLM-13, were sorted by GFP expression by FACS, thus allowing for further culturing and investigation of only the lentivirus infected cells. This would subsequently allow for expanding the cells, in order to perform drug screen on the transduced cells.

3.6.1 Gating strategy for FACS

The gating strategy used for FACS is built upon the same principles as for flow cytometry, presented earlier. To sort the infected cells, the detected events from the flow cytometer were first visualized in an SSC-A/FSC-A scatter plot, where cells were separated from debris, as seen in Figure 15, panel A. Furthermore, a FSC-H/FSC-A scatter plot was utilized to gate the singlets, as this scatter plot allows for excluding doublets, that can affect the data, seen in panel B. Additionally, a gate was set on live cells in panel C, using DRAQ7/FSC-A scatter plot, as this will allow for discriminating between viable and death cells, as the cells were stained with DRAQ7. Finally, a gate was set on GFP positive cells by means of GFP/FSC-A scatter plot, allowing for FACS the GFP positive cells, in panel D. The same gating strategy was used when sorting the other samples.

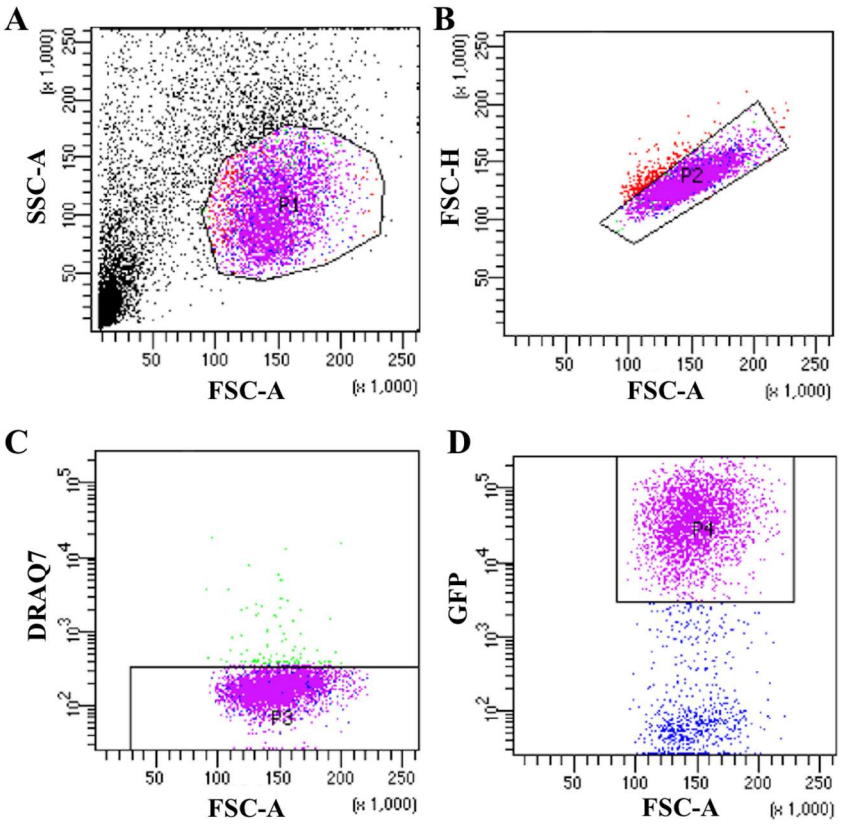

Figure 15. An example of the gating strategy used to sort transduced AML cells. Panel A shows a gating on all events of interest. Panel B shows the gate for singlets. Panel C discriminates between viable and dead cells as determined by DRAQ7 expression. Lastly, panel D shows the gate for GFP positive cells.

3.6.2 FACS of transduced Kasumi-1 and MOLM-13 by GFP expression

Looking at Figure 16, the gating and sorting by GFP positive cells are shown for the two cell lines transduced with either virus. In panel A, Kasumi-1 cells transduced with the lentiviral vector containing pMIN-ERG+85 are seen, whereas in panel B, Kasumi-1 cells transduced with the lentiviral vector containing pMIN are depicted. Similarly, MOLM-13 cells transduced with the lentiviral pMIN-ERG+85 vector are represented in panel C, while MOLM-13 cells transduced with lentiviral vector containing pMIN can be seen in panel D. By gating for GFP expression, using GFP/FSC-A scatter plot, cells positive for infection are represented as the upper purple population, whilst the lower blue population represent non-infected cells. Cell number achieved after FACS for Kasumi-1 cells transduced with the pMIN-ERG+85 vector was $5x10^4$ cells, whereas Kasumi-1 cells transduced with the pMIN vector was only $1x10^4$ cells. For MOLM-13 cells the cell number was $5x10^5$ cells transduced with either virus.

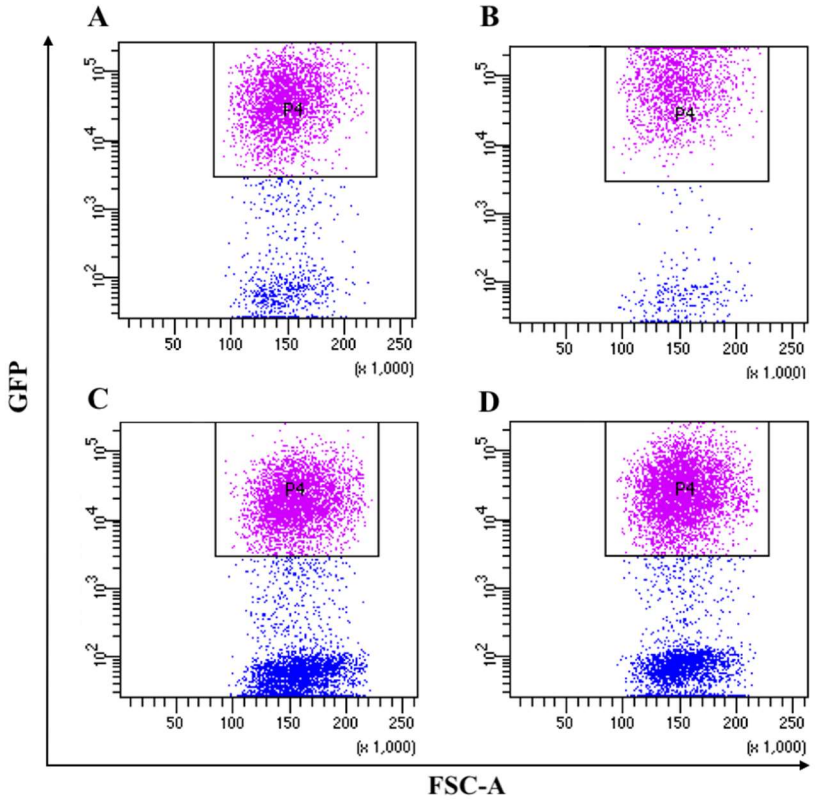

Figure 16. Transduced AML cell lines sorted by GFP expression. Panel A represent Kasumi-1 cells transduced with lentiviral pMIN-ERG+85 vector. In panel B, Kasumi-1 cells transduced with lentiviral vector containing pMIN are presented. In panel C, MOLM-13 cells were transduced with lentiviral vector containing pMIN-ERG+85, panel D presents MOLM-13 cells transduced with lentiviral pMIN vector. Expression of GFP was used to distinguish between infected and non-infected cells using a GFP/FSC-A scatter dot plot.

3.6.3 Flow cytometry analysis of sorted Kasumi-1 and MOLM-13

In order to follow the expression levels of GFP and BFP within the AML cell lines, they were investigated by flow cytometry 10 days after FACS sorting and 28 days post transduction.

The GFP expression in Kasumi-1 cells can be seen in Figure 17, panel A. Cells transduced with pMIN-ERG+85 were expressing 98.07% GFP, whereas 6.22% of the infected cells were expressing BFP, seen in panel B. Moreover, Kasumi-1 cells transduced with the control vector containing pMIN are expressing 97.06% GFP depicted in panel C, where 70.42% were BFP positive within the GFP positive population.

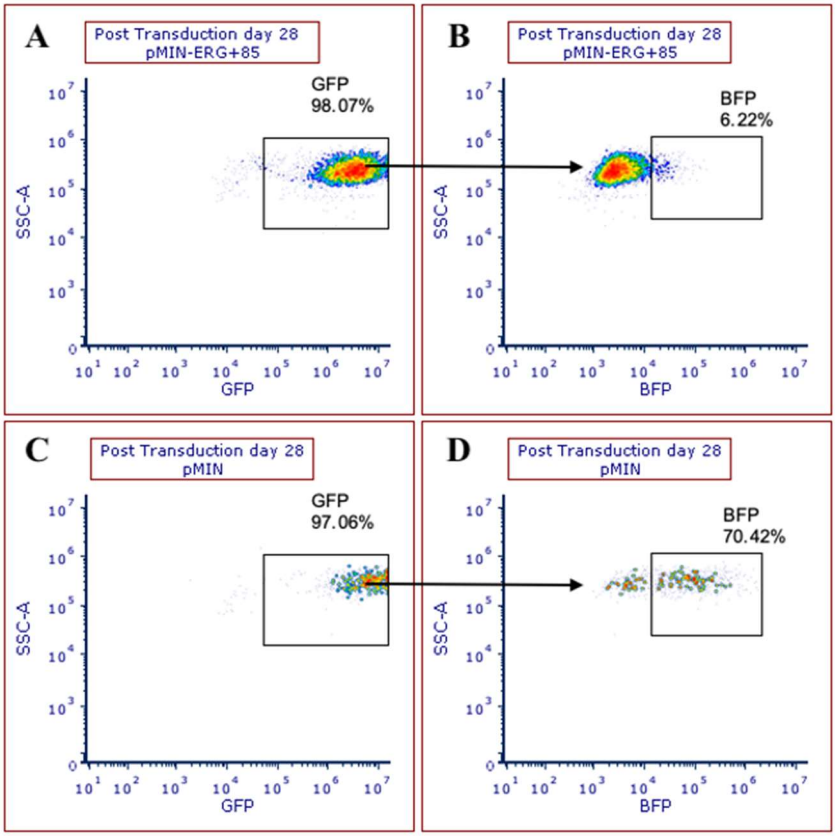

Figure 17. Flow cytometry assessments on day 28 post transduction for Kasumi-1 cells. Panels A and B are cells transduced with lentiviral vector containing pMIN-ERG+85, A shows the GFP expression whereas B shows the BFP expression. In panels C and D cells transduced with the lentiviral vector containing pMIN appear. In panel C, the GFP expression can be seen, while in panel D the BFP expression are present.

Similarly, the GFP expression in MOLM-13 cells can be seen in Figure 18. Cells infected with pMIN-ERG+85 vector seen in panel A is 98.78% and within the GFP positive population 56.92% is BFP positive, as seen in panel B. Cells infected with the control vector containing pMIN were expressing 98.96% GFP, as seen in panel C, and 80.51% of the GFP positive cells were expressing BFP, depicted in panel D.

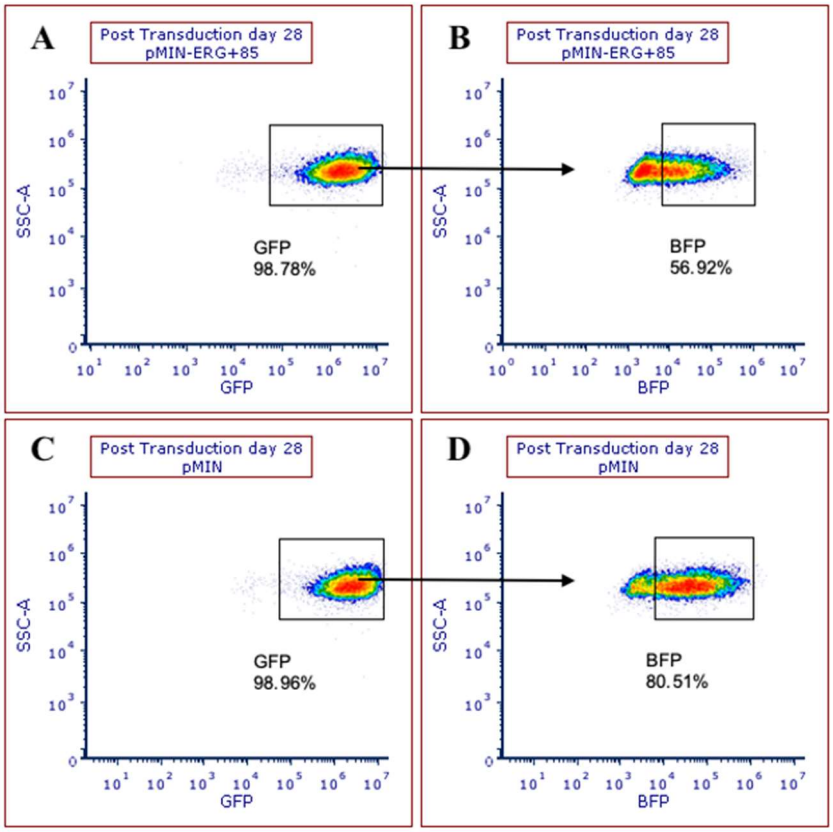

Figure 18. Flow cytometry assessments on day 28 post transduction for MOLM-13 cells. In panels A and B, cells are transduced with the lentiviral vector containing pMIN-ERG+85, where GFP expression can be seen in panel A, BFP expression can be seen in panel B. In panels C and D, cells are transduced with the lentiviral vector containing pMIN. GFP expression appears in panel C, and BFP expression can be seen in panel D.

Common for both AML cell lines was that they showed stable integration of the viral DNA even after 28 days of culturing as observed by continual GFP expression. However, for both Kasumi-1 and MOLM-13 the BFP expression remained higher in cells transduced with the control virus pMIN compared to the pMIN-ERG+85 even 28 days post transduction and after sorting the cells by FACS. Further, the BFP expression seemed to be increasing over time for both cell lines.

3.6.4 Assessment of growth after FACS for Kasumi-1 and MOLM-13

After cells were sorted by FACS, their growth was followed in order to assess when the cell number reached $10x10^6$ cells, which were the required cell number for drug screen on precoated drug plates used in the laboratory. Kasumi-1 and MOLM-13 cells were counted, and the growth was monitored over a period of 14 days. As seen in Figure 19, panel A, Kasumi-1 cells infected

with the viral vector containing pMIN-ERG+85 represents the blue line, starting with a cell number of $5x10^4$ cells, and had after 14 days expanded to $1.411x10^6$ cells. The orange line represents cells infected with the lentiviral vector containing pMIN, these cells started with a cell number of $1x10^4$ cells and had after 14 days expanded to $1.1x10^5$ cells on day 14. In panel B, the growth of MOLM-13 cells can be seen. After cells were sorted, both pMIN-ERG+85 and pMIN infected cells started at a cell number of $5x10^5$ and had after 14 days expanded to $3.19x10^7$ and $2.8x10^7$ cells.

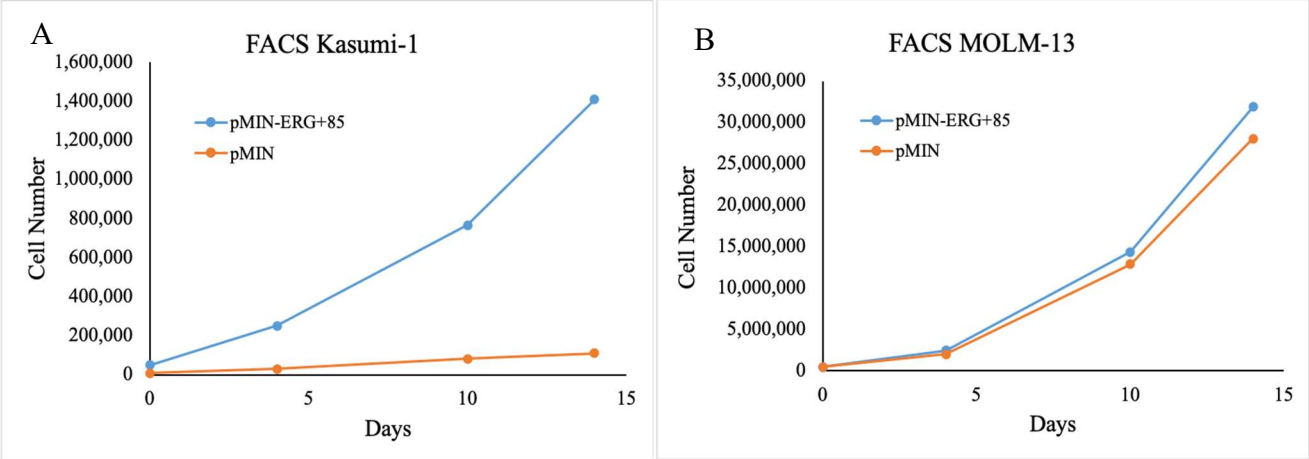

Figure 19. Growth of FACS sorted Kasumi-1 and MOLM-13 cells over 14 days. Panel A shows the growth of sorted Kasumi-1 cells transduced with the lentiviral vector containing pMIN-ERG+85 (blue graph) and pMIN (orange graph). Panel B shows the growth of sorted MOLM-13 cells transduced with the lentiviral vector containing pMIN-ERG+85 (blue graph) and pMIN (orange graph).

Unfortunately, the cell number for Kasumi-1 cells never reached $10x10^6$ cells within the time of the project and therefore setup of the drug screening was not possible to perform. Drug screens could have been performed on MOLM-13 cells, but due to time limitations no further results will be presented in this thesis.

4. Discussion

The purpose of this study was first and foremost to use the lentiviral reporter vector containing pMIN-ERG+85 to transduce the AML cells lines Kasumi-1, KG-1, and MOLM-13, and investigate whether it could be used for identification of drugs targeting LSCs. An effective transduction was seen in Kasumi-1 and MOLM-13 cells, but not in KG-1. Furthermore, the transduced cells were then sorted by positive GFP expression utilizing FACS and subsequently long-term culture of the cells aiming for expansion to $10x10^6$ cells, which is the required cell number for executing the established drug screen setup in the lab. The cells never reached that level within the time period of this project, which is why drug screens utilizing the transduced cell lines unfortunately were not possible to perform in time for this thesis. In the following sections, obtained results from the present study will be discussed.

4.1 Lentiviral transduction of AML cell lines

Lentiviral vectors are useful tools to gene delivery due to their biological features as they can deliver stable gene integration into both dividing and non-dividing cells. In this study it was evident, that the gene product delivered into Kasumi-1 and MOLM-13 cells were stable after 28 days of culturing, which verifies that lentiviral vectors can be used to stable gene product integration. Herein, second generation lentivirus were used, where the HIV-1 pathogen has been modified and thereby only contains four out of nine HIV-1 genes; *gag, pol, rev,* and *tat*. *Gag* encodes structural proteins, where *pol* encodes for reverse transcriptase. *Rev* and *tat* are regulatory genes and are required for viral replication. (46). In the second generation of lentivirus the accessory genes, *vif, vpr, vpu,* and *nef* has been removed for safety issues. Moreover, *env*, which encodes for envelope proteins, has been replaced with another virus glycoprotein, as the env glycoprotein are restricted to bind only receptors represented on $CD4^+$ T cells which narrows the host cell range. To address this host cell issue a replacement of the env to the vesicular stomatitis virus glycoprotein (VSV-G) has been done. VSV-G interacts with phospholipids allowing endocytosis by a broad spectrum of cells (46). However, in this study, the AML cell line, KG-1, showed very little detectable infection when analyzing with flow cytometry, indicating this cell line to be very difficult to transduce with either viruses generated from the vector pMIN-ERG+85 or the control vector pMIN. This can be determined when looking at Figure 10, where very little GFP expression was present, not even at the highest

virus concentration when utilizing polybrene for enhancing the transduction efficiency. The complications with transducing KG-1 cells is in line with a study from 2015, where it was concluded, that the AML cell line, KG-1, were resistant to be infected by retroviruses due to defect binding between VSV-G and KG-1 cells (47), which most likely was the reason for no successful transduction of KG-1 cells in the present study. The use of other envelope glycoproteins to accommodate the binding issue could be the answer here. In a study by *Bell et al.* from 2010, they point out that the endogenous feline virus, RD114 envelope proteins could be more suitable in the use of lentiviral vectors. For instance, RD114 are non-toxic, whereas VSV-G are found to be connected to toxicity (48). In extent of defect binding between VSV-G and KG-1 cells it would be advantageous to use more suitable envelope proteins for future experiments.

4.2 Higher BFP expression in pMIN observed for Kasumi-1 cells

Results from the present study showed a higher expression of BFP signal in cells transduced cells with the control vector containing pMIN than the cells transduced cells with the vector containing pMIN-ERG+85. This was the case when looking at flow cytometry results for the AML cell line Kasumi-1 and quite unexpected as BFP expression was supposed to be an indication of transcription factor binding to ERG+85, and the pMIN vector was lacking ERG+85 enhancer promoter part. In the aforementioned study by Yassin et al., they showed that no BFP fluorescence was detected in transduced leukemia cells with the control vector, pMIN. Vice versa, they showed BFP expression in lentivirally transduced AML cells with the pMIN-ERG+85 vector (35).

With these inconsistent results, one may wonder what has happened. First and foremost, the restriction enzyme analysis seen in Figure 5 verifies the integrity of the purified plasmids from mini prep samples. Additionally, a second restriction enzyme analysis was carried out later in the process, this time on purified midi prep samples to ensure that plasmids pMIN-ERG+85 and pMIN had not been switched around during lentiviral production. The analysis was carried out in the same manner as previously described in section *2.4 Restriction enzyme digestion* and showed the expected digested fragments, which substantiates that the correct vectors were used for the lentivirus production. In addition, the extra bands shown for plasmid pMIN in Figure 5 assumed to be a result of incomplete digestion was not present in the second restriction enzyme analysis. Therefore, there must be other reasons why the BFP expression is higher in pMIN

compared to pMIN-ERG+85. In this study, the lentiviral gene expression is driven by the mCMV promoter. The mCMV promoter is derived from herpes simplex virus and is one of the most commonly used promoters for gene expression. One of the advantages of this promoter is that it is linked to drive high levels of transient gene expression in a broad spectrum of cell types. But at the same time, the CMV promoter is associated with disadvantages, as this type of promoter may be cell type specific, and its promoter activity varies within different cell types (49). Another drawback connected to CMV promoters is their high level of leakiness (50), and this issue may be linked to the mCMV promoter used in this study. With the unexpected high BFP signal in cells transduced with the negative control pMIN lentiviral vector, it can be hypothesized that the mCMV promoter placed in the vicinity of the BFP has led to leaky gene expression, and thereby inducing the observed BFP signal, which is consistent for all the presented results in this study. If the case is a leaky promoter, it could be questionable why the BFP signal are low in Kasumi-1 cells transduced with the lentiviral vector pMIN-ERG+85. The only difference between the two vectors is the presence of the ERG+85 enhancer promoter. Therefore, it could be imagined that ERG+85 enhancer promoter blocks the leakiness from the mCMV promoter, and that the BFP signal may correlate with transcriptional activity of ERG, at least for transduced Kasumi-1 cells transduced with pMIN-ERG+85. As a result of this, it could thereby be explained why a lower BFP signal is observed in cells transduced with the lentiviral vector containing pMIN-ERG+85.

4.3 Abundant BFP signal in MOLM-13 - the ERG negative cell line

In contrast to low BFP expression in Kasumi-1 cells lentivirally transduced with pMIN-ERG+85, a greater expression of BFP was observed in MOLM-13 cells infected with both pMIN-ERG+85 and pMIN. As previously mentioned, MOLM-13 is an AML cell line, and the idea behind using this cell line was that it was not supposed to express *ERG*. Thus, little to no observation of BFP transcriptional activity would be expected to be observed by flow cytometry analysis from the infection with either the lentivirus containing pMIN or the pMIN-ERG+85 vectors. However, the high BFP signal detected in MOLM-13 cells transduced with the lentiviral vectors may be caused by the aforementioned potentially leaky mCMV promoter. A first step towards determining the mechanism causing the high BFP signal, could be to verify the expected presence of ERG within the two cell lines, which could be obtained by performed

western blotting. As mentioned, Kasumi-1 cells are expected to express ERG, whereas MOLM-13 does not.

4.4 Limitations and future perspectives

One of the greatest limitations in this study was associated to the higher BFP expression in cells lentivirally transduced with pMIN than in cells with pMIN-ERG+85. This was not as expected as BFP expression according to the published literature should be an indication of transcriptionally binding activity to ERG+85, and the pMIN vector was lacking the ERG+85 enhancer promoter part. As suggested, the mCMV promoter might have been leaky causing the high BFP expression. For future experiments it might be ideal to try using another promoter. The fact that the Kasumi-1 cells never reached the required cell number for the drug screen after they were sorted with FACS, is also associated with limitations of this project. Here, one could have transduced a higher number of cells, consequently minimizing the period of expansion time after cells were sorted by FACS. Moreover, another limitation was related to the use of KG-1 cells, as they were not suitable for transduction with the produced lentiviruses used in this project. For future experiments, the use of other AML cell lines being able to bind VSV-G is a requirement. Otherwise, if the demand is to transduce KG-1 cells, other envelope glycoproteins should be used.

5. Conclusion

In conclusion the present study manages to produce a lentiviral reporter system containing the vector pMIN-ERG+85. However, integration bias due to a possible leaky CMV promoter made it difficult to isolate LSCs. Moreover, due to time limitations and a shutdown of the laboratories during this study, drug screens were not performed. Before performing drug screens on the lentivirally transduced cells, it is clear that further investigations are needed. For instance, exploring the unexpected transcriptional activity of the vector lacking pMIN-ERG+85 should be performed. When this is clarified the hypothesis, that the expression of BFP under the ERG+85 promoter enhanced in transduced AML cells lines would enable isolation of LSCs, can be investigated.

Bibliography

1. Leukemia Statistics | American Cancer Society - Cancer Facts & Statistics [Internet]. [cited 2020 Feb 17]. Available from: https://cancerstatisticscenter.cancer.org/#!/cancer-site/Leukemia
2. Shallis RM, Wang R, Davidoff A, Ma X, Zeidan AM. Epidemiology of acute myeloid leukemia: Recent progress and enduring challenges. Blood Rev. 2019;36:70–87.
3. Döhner H, Weisdorf DJ, Bloomfield CD. Acute myeloid leukemia. N Engl J Med. 2015;373(12):1136–52.
4. Khwaja A, Bjorkholm M, Gale RE, Levine RL, Jordan CT, Ehninger G, et al. Acute myeloid leukemia. 2016;(March).
5. Crane GM, Jeffery E, Morrison SJ. Adult haematopoietic stem cell niches. Nat Rev Immunol [Internet]. 2017;17(9):573–90. Available from: http://dx.doi.org/10.1038/nri.2017.53
6. Aggarwal R, Lu J, J. Pompili V, Das H. Hematopoietic Stem Cells: Transcriptional Regulation, Ex Vivo Expansion and Clinical Application. Curr Mol Med. 2011;12(1):34–49.
7. Nakajima H. Role of transcription factors in differentiation and reprogramming of hematopoietic cells. Keio J Med. 2011;60(2):47–55.
8. Tabe Y, Konopleva M. Advances in understanding the leukaemia microenvironment. Br J Haematol. 2014;164(6):767–78.
9. He N, Zhang L, Cui J, Li Z. Bone Marrow Vascular Niche: Home for Hematopoietic Stem Cells. Bone Marrow Res. 2014;2014:1–8.
10. Sugiyama T, Kohara H, Noda M, Nagasawa T. Maintenance of the Hematopoietic Stem Cell Pool by CXCL12-CXCR4 Chemokine Signaling in Bone Marrow Stromal Cell Niches. Immunity. 2006;25(6):977–88.
11. Rosenbauer F, Tenen DG. Transcription factors in myeloid development: Balancing differentiation with transformation. Nat Rev Immunol. 2007;7(2):105–17.
12. Pabst T, Mueller BU. Transcriptional dysregulation during myeloid transformation in AML. Oncogene. 2007;26(47):6829–37.
13. Kunchala P, Kuravi S, Jensen R, McGuirk J, Balusu R. When the good go bad: Mutant NPM1 in acute myeloid leukemia. Blood Rev [Internet]. 2018;32(3):167–83. Available from: https://doi.org/10.1016/j.blre.2017.11.001
14. Horton SJ, Huntly BJP. Recent advances in acute myeloid leukemia stem cell biology.

Haematologica. 2012;97(7):966–74.

15. Grafone T, Palmisano M, Nicci C, Storti S. An overview on the role of FLT3-tyrosine kinase receptor in acute myeloid leukemia: Biology and treatment. Oncol Rev. 2012;6(1):64–74.
16. Gu X, Ebrahem Q, Mahfouz RZ, Hasipek M, Enane F, Radivoyevitch T, et al. Leukemogenic nucleophosmin mutation disrupts the transcription factor hub that regulates granulomonocytic fates. J Clin Invest. 2018;128(10):4260–79.
17. Tsapogas P, Mooney CJ, Brown G, Rolink A. The cytokine Flt3-ligand in normal and malignant hematopoiesis. Int J Mol Sci. 2017;18(6).
18. Zheng R, Friedman AD, Levis M, Li L, Weir EG, Small D. Internal tandem duplication mutation of FLT3 blocks myeloid differentiation through suppression of C/EBPα expression. Blood. 2004;103(5):1883–90.
19. Austin R, Smyth MJ, Lane SW. Harnessing the immune system in acute myeloid leukaemia. Crit Rev Oncol Hematol [Internet]. 2016;103(April):62–77. Available from: http://dx.doi.org/10.1016/j.critrevonc.2016.04.020
20. Wichmann C, Chen L, Heinrich M, Baus D, Pfitzner E, Zörnig M, et al. Targeting the oligomerization domain of ETO interferes with RUNX1/ETO oncogenic activity in t(8;21)-positive leukemic cells. Cancer Res. 2007;67(5):2280–9.
21. Al-Harbi S, Aljurf M, Mohty M, Almohareb F, Ahmed SOA. An update on the molecular pathogenesis and potential therapeutic targeting of AML with t(8;21)(q22;q22.1);RUNX1-RUNX1T1. Blood Adv. 2020;4(1):229–38.
22. Watts J, Nimer S. Recent advances in the understanding and treatment of acute myeloid leukemia. F1000Research. 2018;7(0).
23. Kumar CC. Genetic abnormalities and challenges in the treatment of acute myeloid Leukemia. Genes and Cancer. 2011;2(2):95–107.
24. De Kouchkovsky I, Abdul-Hay M. 'Acute myeloid leukemia: A comprehensive review and 2016 update'. Blood Cancer J. 2016;6(7).
25. Döhner H, Estey E, Grimwade D, Amadori S, Appelbaum FR, Ebert BL, et al. Global Acute Myeloid Leukemia Epidemiology and Patient Flow Analysis 2016. Blood. 2017;129(4):424–48.
26. Talati C, Sweet K. Recently approved therapies in acute myeloid leukemia: A complex treatment landscape. Leuk Res [Internet]. 2018;73(September):58–66. Available from: https://doi.org/10.1016/j.leukres.2018.09.001

27. Chopra M, Bohlander SK. The cell of origin and the leukemia stem cell in acute myeloid leukemia. Genes Chromosom Cancer. 2019;58(12):850–8.
28. Roboz GJ, Guzman M. Acute myeloid leukemia stem cells: Seek and destroy. Expert Rev Hematol. 2009;2(6):663–72.
29. Laverdière I, Boileau M, Neumann AL, Frison H, Mitchell A, Ng SWK, et al. Leukemic stem cell signatures identify novel therapeutics targeting acute myeloid leukemia. Blood Cancer J [Internet]. 2018;8(6). Available from: http://dx.doi.org/10.1038/s41408-018-0087-2
30. Eppert K, Takenaka K, Lechman ER, Waldron L, Nilsson B, Van Galen P, et al. Stem cell gene expression programs influence clinical outcome in human leukemia. Nat Med [Internet]. 2011;17(9):1086–94. Available from: http://dx.doi.org/10.1038/nm.2415
31. Thomas D, Majeti R. Biology and relevance of human acute myeloid leukemia stem cells. Blood. 2017;129(12):1577–85.
32. Marcucci G, Maharry K, Whitman SP, Vukosavljevic T, Paschka P, Langer C, et al. High expression levels of the ETS-related gene, ERG, predict adverse outcome and improve molecular risk-based classification of cytogenetically normal acute myeloid leukemia: A cancer and leukemia group B study. J Clin Oncol. 2007;25(22):3337–43.
33. Diffner E, Beck D, Gudgin E, Thoms JAI, Knezevic K, Pridans C, et al. Erratum: Activity of a heptad of transcription factors is associated with stem cell programs and clinical outcome in acute myeloid leukemia (Blood (2013) 121:12 (2289-2300)). Blood. 2014;123(18):2901.
34. Thoms JAI, Birger Y, Foster S, Knezevic K, Kirschenbaum Y, Chandrakanthan V, et al. ERG promotes T-acute lymphoblastic leukemia and is transcriptionally regulated in leukemic cells by a stem cell enhancer. Blood. 2011;117(26):7079–89.
35. Yassin M, Aqaqe N, Yassin AA, van Galen P, Kugler E, Bernstein BE, et al. A novel method for detecting the cellular stemness state in normal and leukemic human hematopoietic cells can predict disease outcome and drug sensitivity. Leukemia [Internet]. 2019;2061–77. Available from: http://dx.doi.org/10.1038/s41375-019-0386-z
36. Marshall JC, Kelch RP. Intravenous infusion of bone marrow in patients receiving radiation and chemotherapy. 1986;
37. Lee JJ, Chung IJ, Park MR, Ryang DW, Park CS, Kim HJ. Increased angiogenesis and Fas-ligand expression are independent processes in acute myeloid leukemia. Leuk Res. 2001;25(12):1067–73.
38. Hecht A, Nowak D, Nowak V, Hanfstein B, Faldum A, Büchner T, et al. High expression of

the Ets-related gene (ERG) is an independent prognostic marker for relapse-free survival in patients with acute promyelocytic leukemia. Ann Hematol. 2013;92(4):443–9.

39. Wei AH, Tiong IS. Blood Spotlight and venetoclax bring new hope to AML. Blood. 2017;130(23):2469–75.
40. Stone RM, Mandrekar SJ, Sanford BL, Laumann K, Geyer S, Bloomfield CD, et al. Midostaurin plus chemotherapy for acute myeloid leukemia with a FLT3 Mutation. N Engl J Med. 2017;377(5):454–64.
41. Juárez-Salcedo LM, Desai V, Dalia S. Venetoclax: Evidence to date and clinical potential. Drugs Context. 2019;8:1–13.
42. Pollyea DA, Amaya M, Strati P, Konopleva MY. Venetoclax for AML: Changing the treatment paradigm. Blood Adv. 2019;3(24):4326–35.
43. Agilent Technlogies. XL1-Blue Competent Cells, Manual Catalog #200249. 2004;10–1. Available from: http://www.chem-agilent.com/pdf/strata/200249.pdf
44. Chung KY, Rim KW, Lee JH. QIAGEN® Plasmid Purification Handbook. Lect Notes Electr Eng. 2012;120 LNEE(April):445–54.
45. Wayne AS, FitzGerald DJ, Kreitman RJ, Pastan I, Walsh MJ, Dodd JE, et al. Improve lentiviral production using Lipofectamine 3000 reagent Invitrogen™. Abcam [Internet]. 2012;12(8):452–69. Available from: http://dx.doi.org/10.1016/j.bbagrm.2013.01.008%5Cnhttp://www.ncbi.nlm.nih.gov/pubmed/25234619%5Cnhttp://biochemsoctrans.org/lookup/doi/10.1042/BST20120057%5Cnhttp://dx.doi.org/10.1038/icb.2011.20%5Cnhttp://dx.doi.org/10.1038/srep12444%5Cn10.1038/srep12444
46. Milone MC, O'Doherty U. Clinical use of lentiviral vectors. Leukemia [Internet]. 2018;32(7):1529–41. Available from: http://dx.doi.org/10.1038/s41375-018-0106-0
47. Boso G, Somia N V. Characterization of resistance to rhabdovirus and retrovirus infection in a human myeloid cell line. PLoS One. 2015;10(3):1–17.
48. Bell AJ, Fegen D, Ward M, Bank A. RD114 envelope proteins provide an effective and versatile approach to pseudotype lentiviral vectors. Exp Biol Med. 2010;235(10):1269–76.
49. Damdindorj L, Karnan S, Ota A, Hossain E, Konishi Y, Hosokawa Y, et al. A comparative analysis of constitutive promoters located in adeno-associated viral vectors. PLoS One. 2014;9(8):1–10.
50. Ede C, Chen X, Lin M-Y, Yvonne YC. Quantitative Analyses of Core Promoters Enable

Precise Engineering of Regulated Gene Expression in Mammalian Cells. Nat Med. 2010;16(4):438–45.